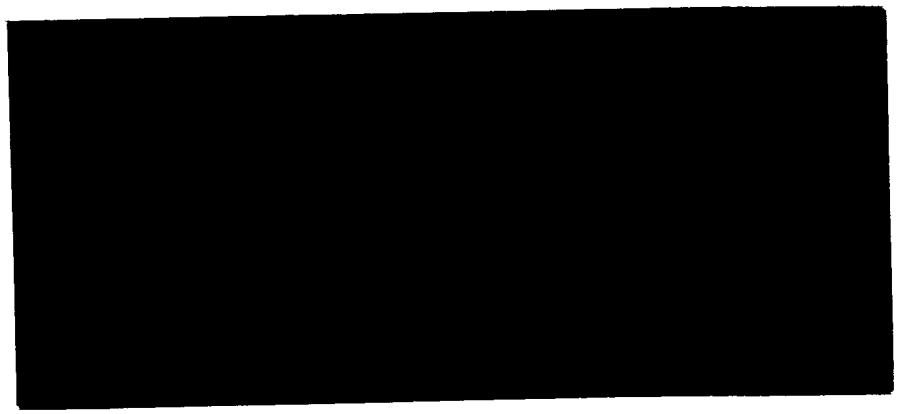

GPO PRICE $ _____

CFSTI PRICE(S) $ _____

Hard copy (HC) $3.00

Microfiche (MF) .75

ff 653 July 65

FACILITY FORM 602

N66-22823 (ACCESSION NUMBER) — (THRU) 1

65 (PAGES) — (CODE)

CR-21242 (NASA CR OR TMX OR AD NUMBER) — 03 (CATEGORY)

THERMO ELECTRON

ENGINEERING CORPORATION

Thermo Electron Engineering Corporation, 85 First Avenue, Waltham, Massachusetts 02154

Contract No. 951263 Report No. TE 69-66

FIRST QUARTERLY REPORT

SOLAR THERMIONIC

GENERATOR DEVELOPMENT

This work was performed for the Jet Propulsion Laboratory, California Institute of Technology, sponsored by the National Aeronautics and Space Administration under Contract NAS7-100.

March 1966

by

Pierre J. Brosens

Prepared for

Jet Propulsion Laboratory

Pasadena, California

TABLE OF CONTENTS

INTRODUCTION

This document constitutes the First Quarterly Report of the work being performed under Thermo Electron's contract No. 951263 with the Jet Propulsion Laboratory.

The objectives of this program are two-fold, and are to be reached under two task efforts; they are:

I. To develop a converter of the design used under Task II of Contract No. 950671, which is capable of delivering a power output of 20 watts/cm^2 at one volt, with a minimum measured efficiency of 16%.

II. To develop a prototype structure of a 14% efficient multiconverter generator capable of operation in cislunar space with a concentrator 9.5 ft. in diameter and which uses the converters developed under Task I.

Task I centers on the iterative construction of 9 engineering models of a solar energy thermionic converter. The aim of the first model is to partially duplicate the best converter developed under Task II of Contract No. 950671. The second and third are principally geared to the incorporation of a modification in the heat transfer path of the collector-radiator structure to assure efficient and reliable heat transfer. The fourth and fifth are intended to effect a change in the materials of the convoluted emitter structure whereby the entire structure will be made of rhenium. The sixth and seventh converters will study two new collector materials and the eighth will be a final prototype incorporating all the features found to improve performance in the course of the work. The ninth prototype will duplicate the eighth except that the interelectrode spacing will be increased to 2 mils in order to make a performance comparison.

Task II involves a generator flux analysis, a shielding evaluation, and a mock-up environmental test based on the design of a selected generator design. The analysis will determine the best number of converters to match the converter heat requirements to the available solar energy, the optimum cavity aperture size, the required adjustments of surface emissivitiy and absorptivity values to insure even flux distribution, and the effects of changes in emitter temperature and heat input on flux distribution within the generator. The shielding test is primarily intended to verify design assumptions on shielding heat losses, and to select a preferred shield configuration. The mock-up environmental tests will be conducted to explore all areas of possible structural weakness to vibration, shock, acceleration and acoustical environments, and effect the design changes indicated.

This report covers progress for the period November 22, 1965 to March 1, 1966.

SUMMARY

During the first quarter, the first two engineering models, T-201 and T-202, have been fabricated, and the first one has been tested. Test results indicate that the interelectrode spacing achieved in this converter was of the order of 1.4 mil instead of the desired value of 1 mil. As a result, its performance has not equalled that of the converters tested under Contract No. 950671. Preliminary tests on Converter T-202 do not reflect a similar loss in performance. It is suspected that the difficulty is related to a lack of good mechanical alignment in the assembly of T-201 and also to a loss of flatness in the converter electrodes which results from the existing etching processes. Since the electrodes of converter T-203 will be particularly flat, it is expected that the tests of this converter will tend to confirm the above suspicions.

Under Task II, all analytic work has been completed. Digital computer results were obtained for 137 different combinations of cavity emissivities, heat input, emitter temperature, aperture size, and number of converters. This data, combined with the performance of a selected converter from Task I, will provide accurate predictions of generator performance. The most significant results derived from the computations are:

1. Even thermal distribution can be achieved by etching or grooving the heated surface of only one family of converters in the generator.
2. Once a generator is thermally balanced, it will remain so even under pronounced changes in the emitter temperature of the converters, and/or in the heat input to the generator cavity.

This last result is surprising, and judged to be of substantial significance as far as the future of solar thermionics is concerned: many problems had been foreseen regarding the control of generator operation because it had been assumed that thermal balance could be achieved at only particular combinations

of emitter temperature and heat input. This has now been demonstrated, at least analytically, not to be the case: thermal balance, and hence, predictable generator output can be expected from a generator that has been thermally balanced at only one operating condition.

1.0 CONVERTER DEVELOPMENT

1.1 Converter Design

The features for the successive converter prototypes to be fabricated under Task I are summarized in Table 1. During this reporting period, the first three of these prototypes, T-201 to T-203 were designed. The designs are presented in Figures 1 and 2. The drawings present four different designs numbered I to IV. This notation corresponds to that used in the bottom entry of Table 1. Thus, the design of converter T-201 is the design I. As specified in the Statement of Work, this design includes the collector structure of the converter T-100 developed under the previous contract No. 950671. The main feature of converters T-202 and 203 is a modified collector-radiator structure which minimizes the effect of a braze interface on collector temperature distribution. Design III, which corresponds to converters T-204 to T-208, will include as a principal feature an all-rhenium emitter structure. Design IV, that of converter T-209, will involve a modification of the re-entrant emitter structure to provide an interelectrode spacing of 2 mils. At this point, only designs I and II have been finalized. The other designs are tentative and for planning purposes only.

1.2 Component Development

1.2.1 Collector-Radiator Model

In order to evaluate the redesigned braze interface in the collector structure for the converters of Designs II, III and IV, an experimental collector-radiator structure was designed, fabricated and tested. It was also intended to test this structure so as to evaluate the heat load that the radiator can dispose of as a function of collector temperature.

TABLE 1. SUMMARY OF PROTOTYPE FEATURES

Feature \ Prototype	T-201	T-202	T-203	T-204	T-205	T-206	T-207	T-208	T-209
Hohlraum L/D	8	8	8	8	8	8	8	8	8
Emitter Material	Re	Re	Re	Re	Re	Re	Re	Re	Re
Emitter Fabrication	.020 G. Bond	.020 G. Bond	.020 G. Bond	.060	.060	.060	.060	.060	.060
Emitter Preparation	Electrop. & Thermal	id.	id.	id.	id.	id.	id.	id.	id.
Collector Material	Mo	Mo	Mo	Mo	Mo				
Collector Preparation	Ground	Chem.	Chem.						
Collector Area, cm^2	2.50	2.50	2.50	2.50	2.50	2.50	2.50	2.50	2.50
Collector Lateral Area, cm^2	2.00	2.00	2.00	2.00	2.00	2.00	2.00	2.00	2.00
Interelectrode Spacing, in.	.001	.001	.001	.001	.001	.001	.001	.001	.002
Lateral Electrode Spacing, in.	.006	.006	.006	.006	.006	.006	.006	.006	.006
Radiator Area, cm^2	113	113							
Number of Rhenium Sleeves	0	0	0	3	3	3	3	3	2
Reservoir Extension, in.	1.1	1.1	1.1	1.1	1.1	1.1	1.1	1.1	1.1
Emitter Shielding	2 Ta	2 Ta							
Weight, bare, gms.	—								
Weight, instrumented, gms.	—								
Design Reference	I	II	II	III	III	III	III	III	IV

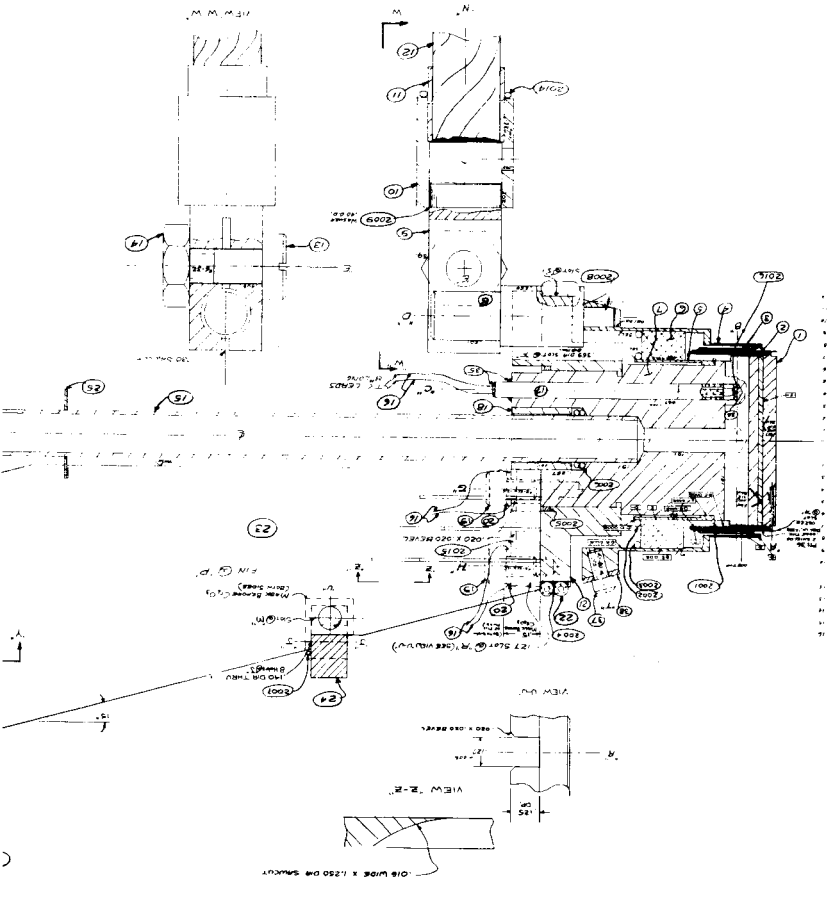

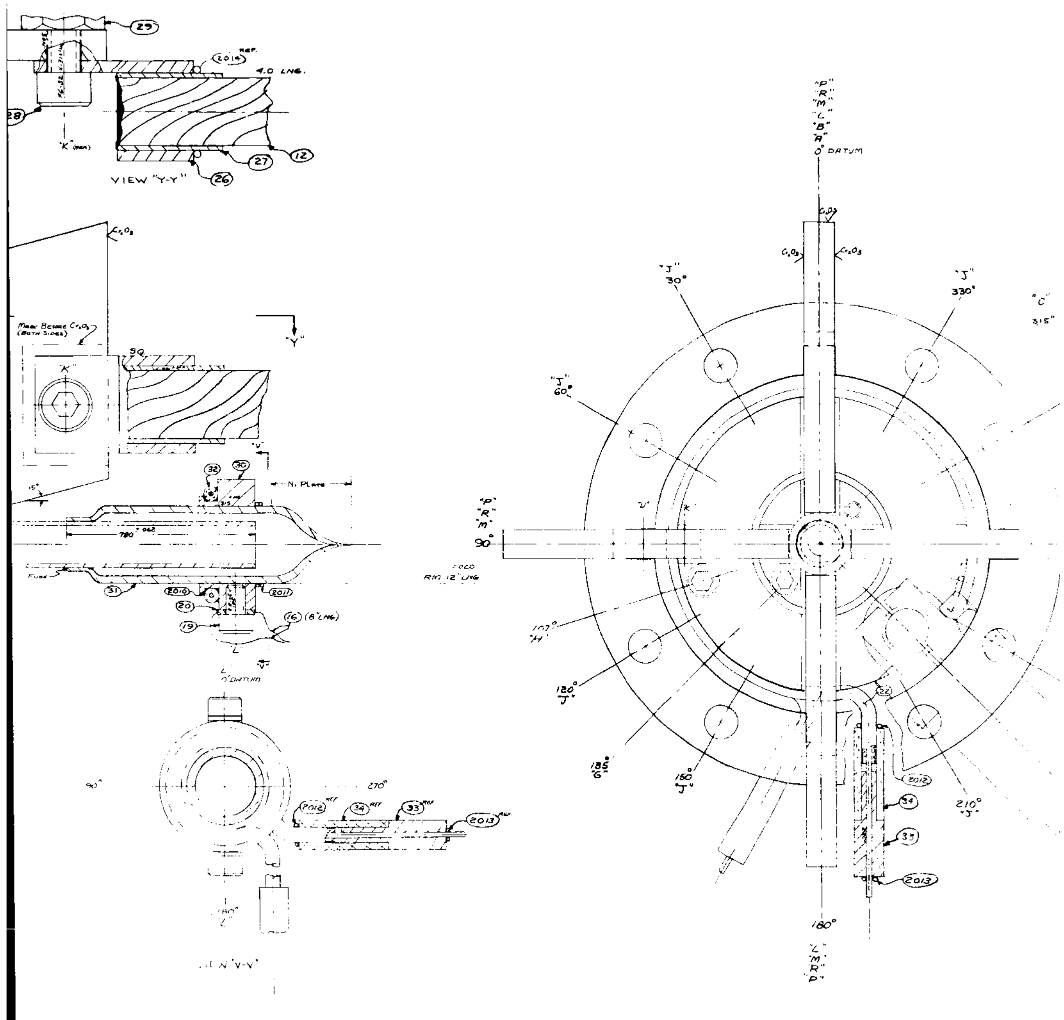

29
2014 REF.
4.0 LNG.
"K" (MAX)
27
12
VIEW "Y-Y"
26
"Y"
"V"
N. PLATE
.780
31
2010
2011
20
19
16 (8" LNG)
0° DATUM
270°
2012 REF
34 REF
33 REF
2013 REF
180°
"P"
"R"
"M"
"L"
"B"
"A"
0° DATUM
"J" 30°
"J" 330°
"C" 315°
"J" 60°
"P" "R" "M" 90°
107° "H"
120° "J"
135° "G"
150° "J"
210° "J"
22
2012
34
33
2013
180°
"L" "M" "R" "P"

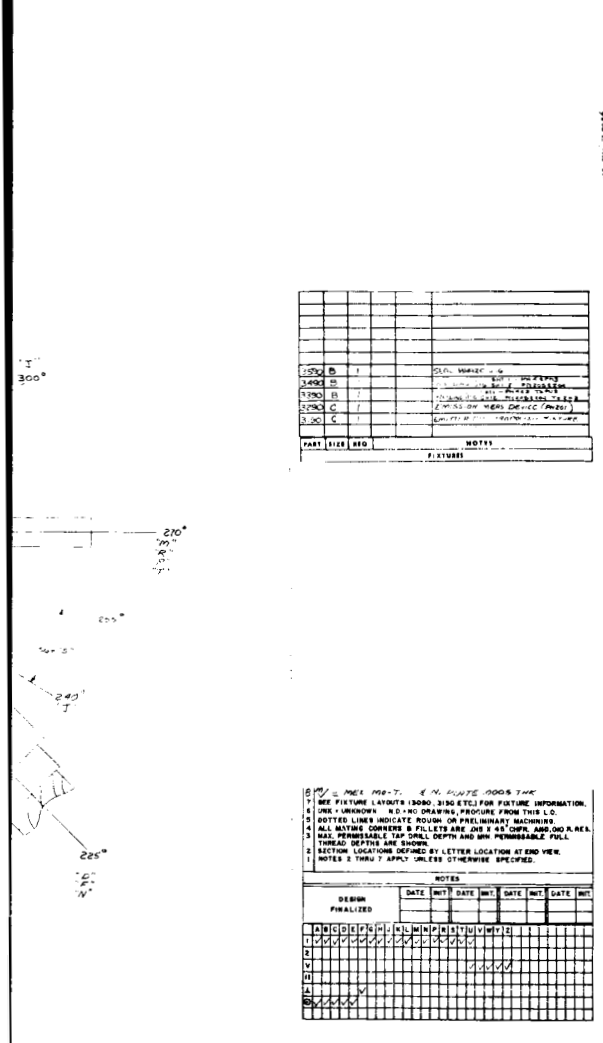

Figure 1.

T-200 Converter Layout - Design IV

3

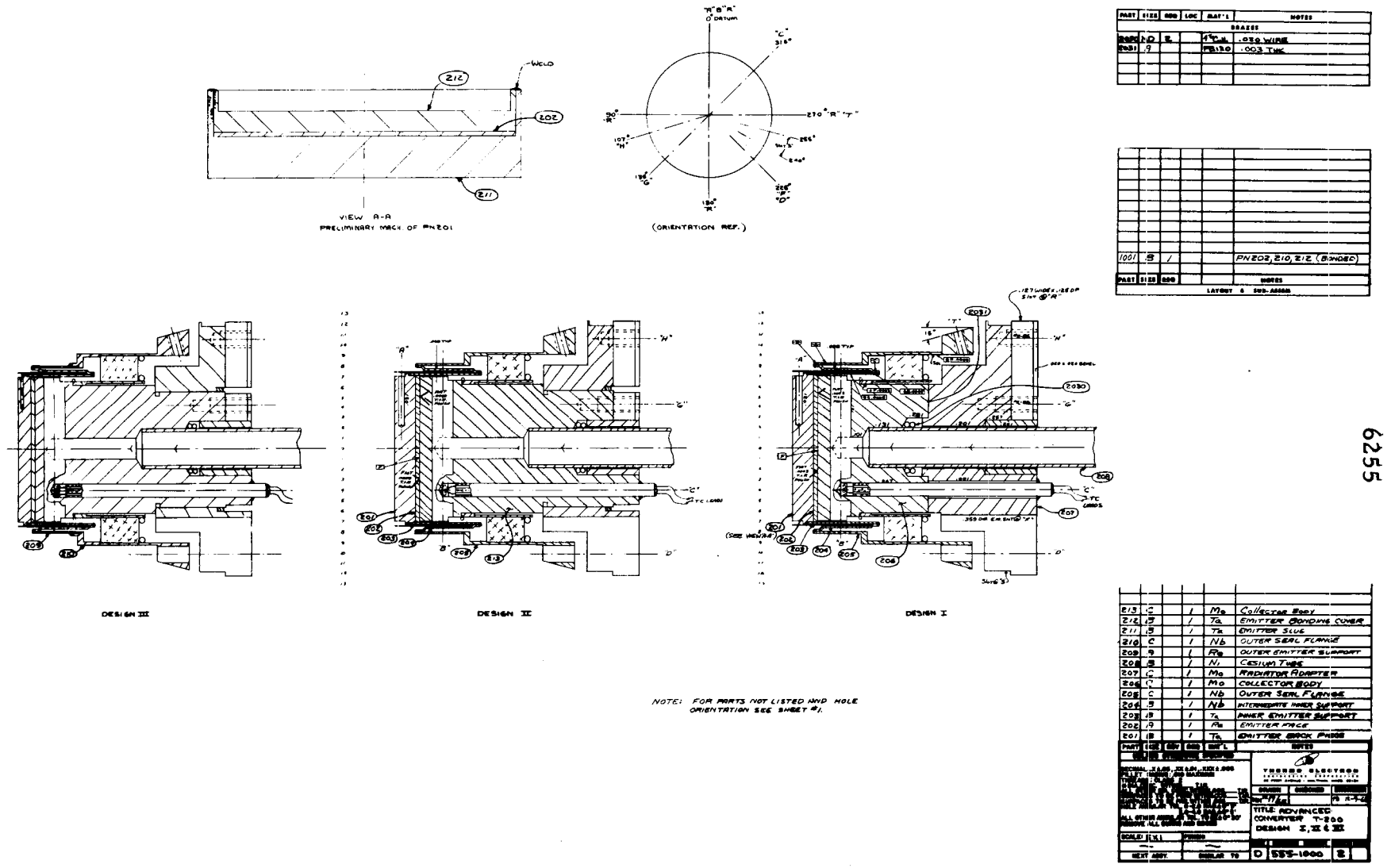

Figure 2. T-200 Layout Detail - Designs I, II and III.

Figure 3 is a drawing of the collector-radiator model fabricated. It reproduces the radiator structure of the TE-100 converter built under contract 950671, and it includes a collector body with a cylindrical braze (2002) in the area of heat transfer to the radiator support. As may be seen, the collector-radiator structure tested reproduces that of the recommended T-202 design. The completed collector-radiator model is shown in Figure 4. As a novel development, the radiator fins were coated with zirconium carbide.

The radiator-collector model was tested at heat input levels of 110, 210, and 310 watts. The design input value is 158.5 watts. The temperature levels achieved are given in Figures 5 and 6. Figure 5 gives the temperature rise produced when the only heat input is that of radiation from the electron bombardment of filament. Analysis of this data shows that the filament contribution is 10 watts. Figure 6 gives the temperature levels at total heat input values of 110, 210, and 310 watts. The only abnormal result from this run is the relatively high reservoir temperature level. In an attempt to reduce this temperature, a shield was placed along the tubulation to isolate the cesium tube from radiation by the radiator fins. This resulted in a still higher temperature level at the reservoir because, as it became apparent, the cesium tube loses more heat by its own radiation than it receives from the radiator fins. In another attempt the shield was removed and the copper pinch off of the reservoir was painted with a black silicone paint. This coating lowered the reservoir temperature by more than 100°C. Such a result indicates that any problem with overheating of the cesium reservoir should be easily overcome by the application of a coating to the reservoir, or by a reduction in the cross section of the reservoir tubulation.

Figure 6 shows that a heat input equal to the design value of 158.5 watts (interelectrode radiation = 33.5 w, cesium conduction 24.0 w, electron heating

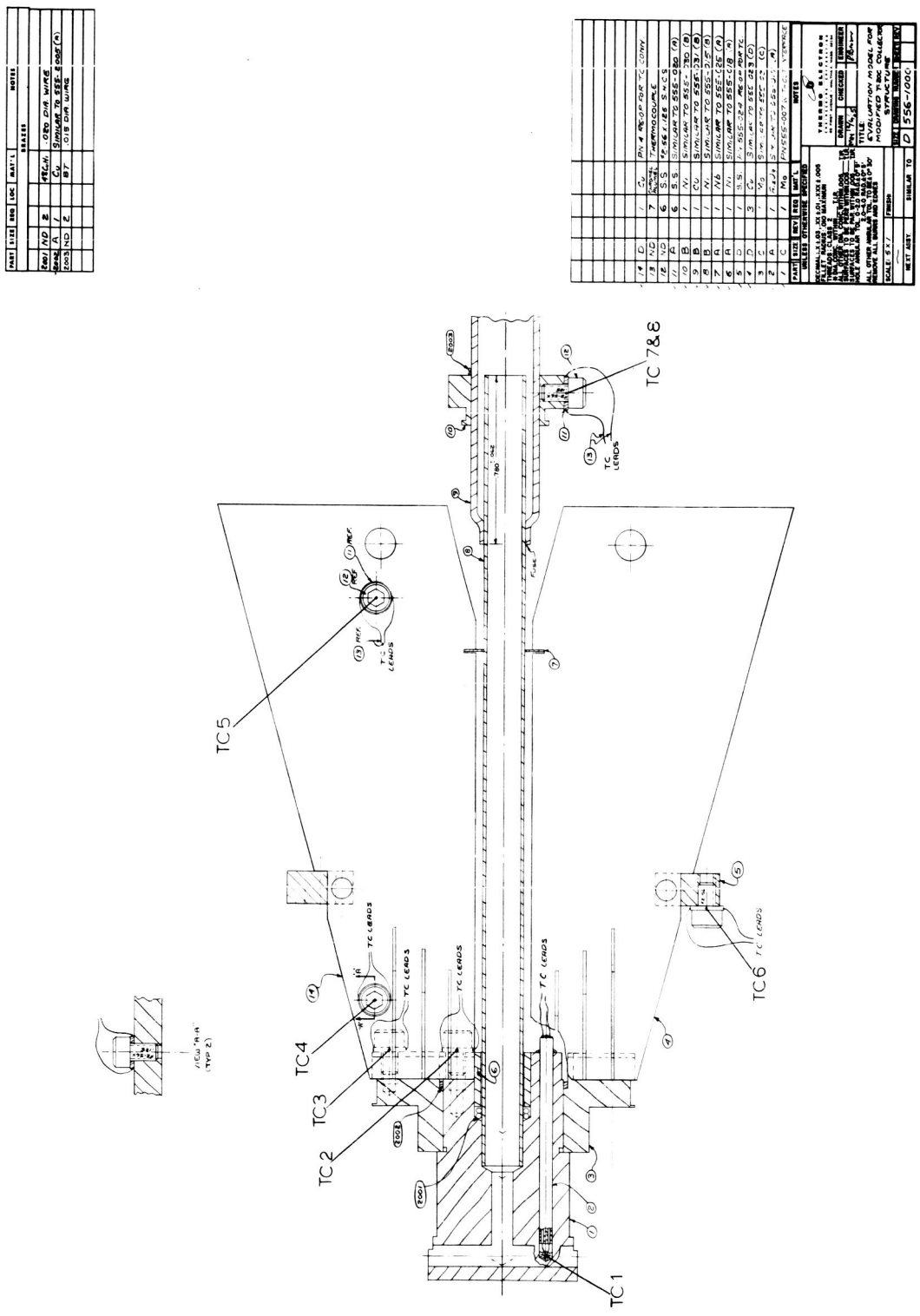

Figure 3. Layout of Collector-Radiator Model.

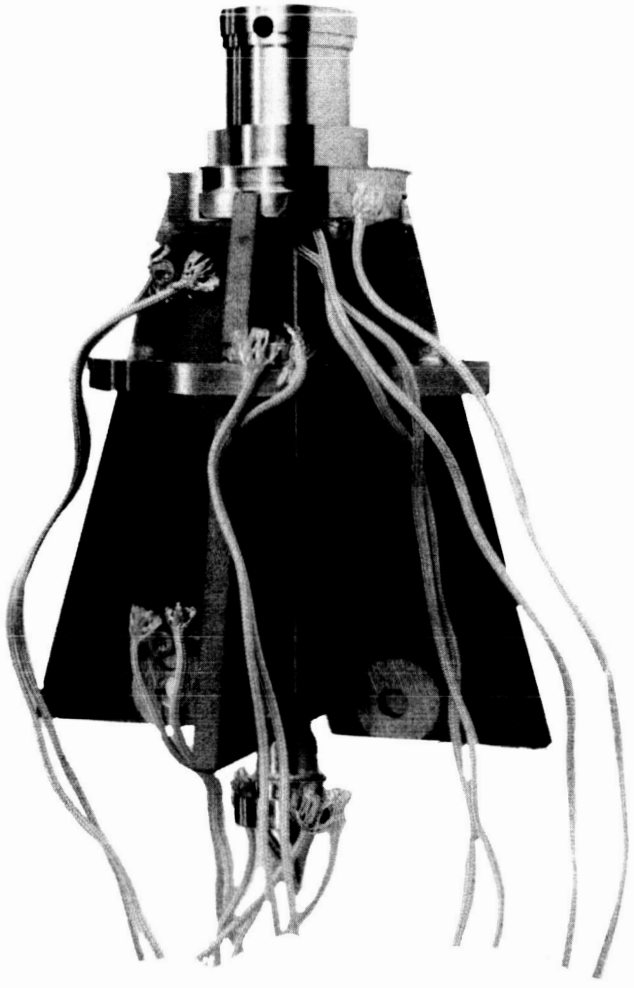

Figure 4. View of Assembled Collector-Radiator Model.

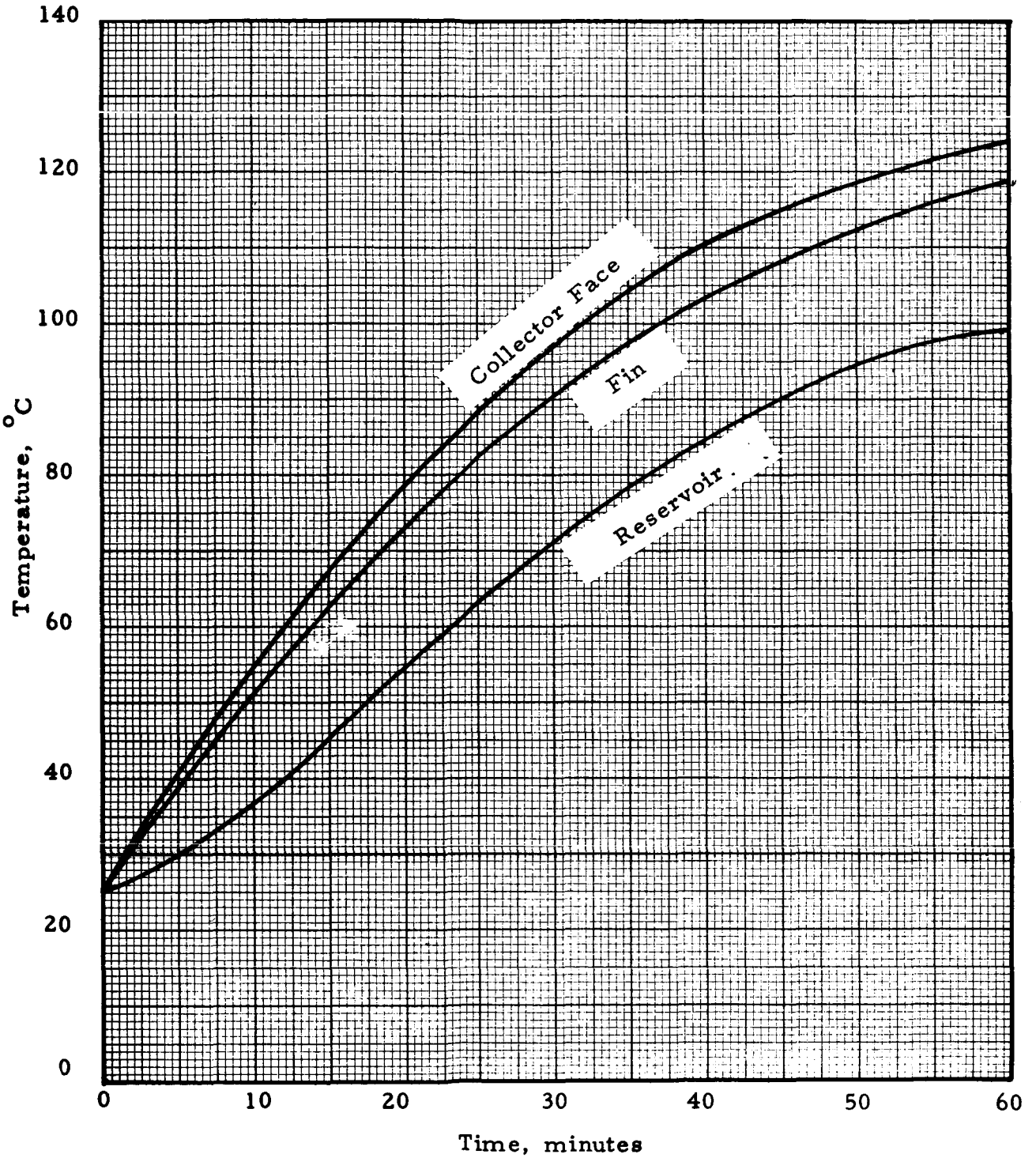

Figure 5. Collector-Radiator Model — Run No. 1.

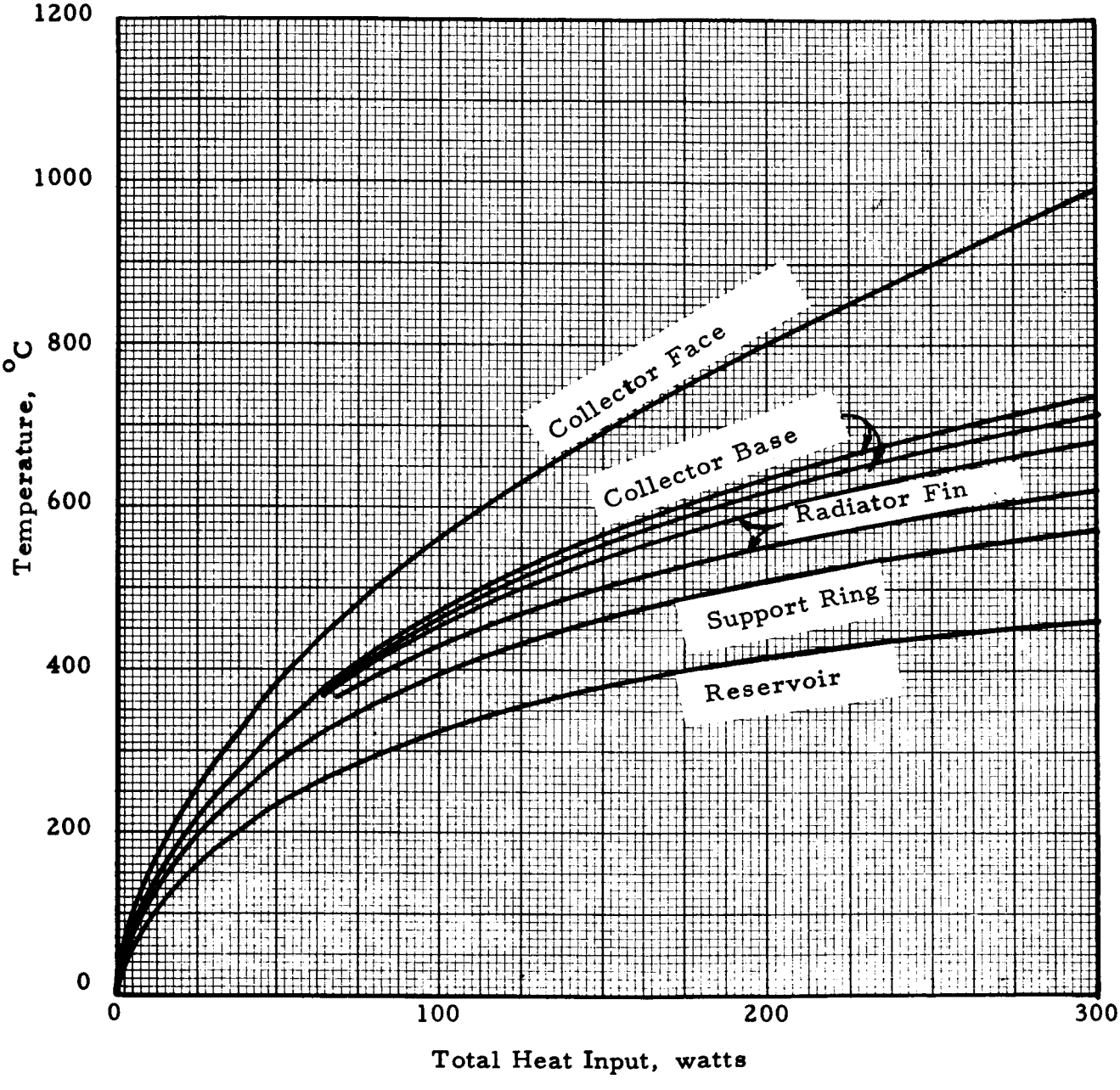

Figure 6. Collector-Radiator Model — Run No. 2.

at 20 amp/cm^2, 1 volt = 86 w, radiation from sleeve = 15 w, the conduction from the emitter support is assumed to be cancelled by radiation from the connecting leads) yields a collector face temperature of 1013°K which is in line with the previously observed optimum collector temperature for converter TE-103 at 1 volt of 1015°K. Since it appeared that the radiator size of the model tested is as close to that required for converter T-202 as a collector-radiator model test of the type performed can actually predict, converter T-202 was fabricated with a radiator of that size using a zirconium carbide coating on the fins.

1.2.2 All-Rhenium Emitter Structure

Prior to the fabrication of the converter models of Design III and IV, it is intended to fabricate and test a prototype of their all-rhenium emitter structure to test the ability of such a structure to withstand cycling to elevated temperature. Work on this item has not yet been initiated except for procurement of all the required rhenium material.

1.3 Converter Fabrication

The converter assembly techniques used are the same as those that were used in the fabrication of converters under JPL contract 950671.

Figures 7, 8, and 9 illustrate the differences in the collector structure which have resulted from the redesign effort under the present program. Figure 7 shows the parts for the collector structure of converter T-201 before assembly. Figure 8 shows the same parts after brazing with palladium. In spite of its poor appearance, the braze of Figure 8 is leaktight, and previous experience has shown that once this braze is leaktight it will remain so. To obtain a leaktight braze has presented a problem however. In the first attempt, two collector assemblies were brazed and both leaked due to excessive alloying of the braze with the niobium seal flange. Examination of the constitution diagram of the

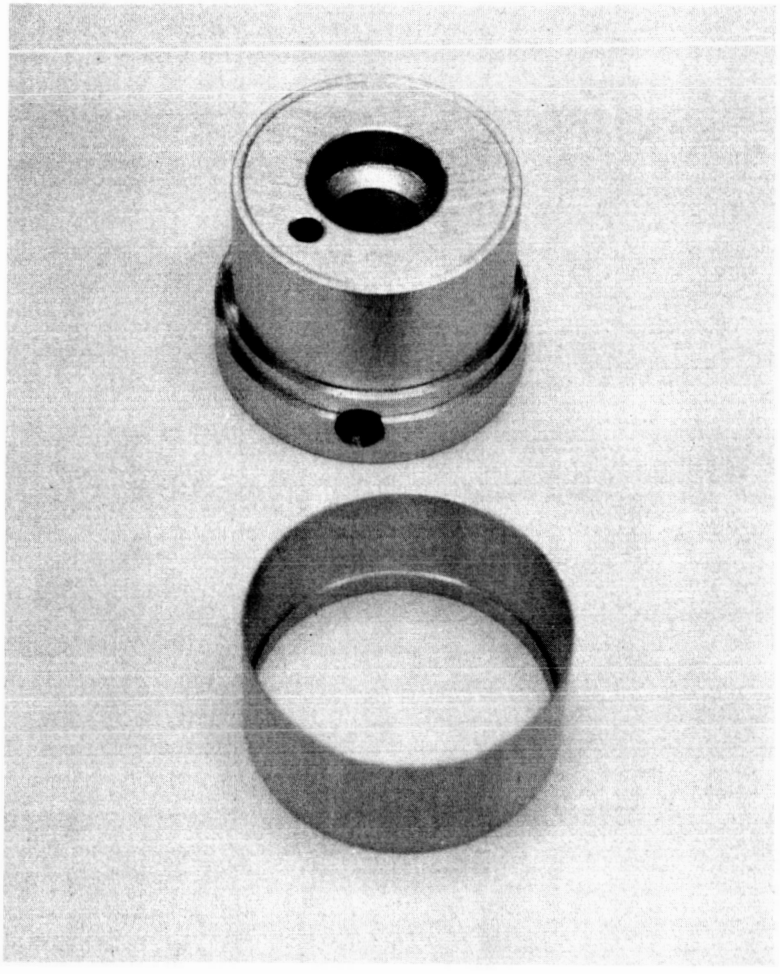

Figure 7. Parts for T-201 Collector Subassembl

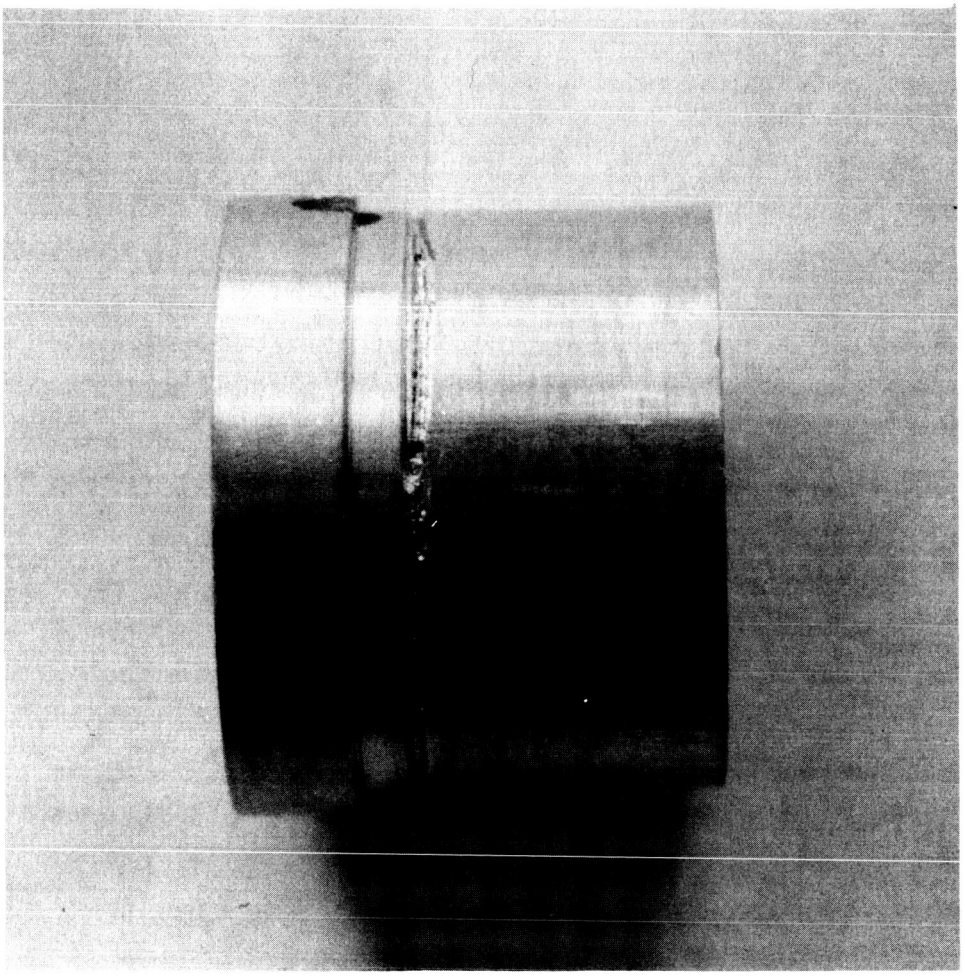

Figure 8. T-201 Collector Subassembly.

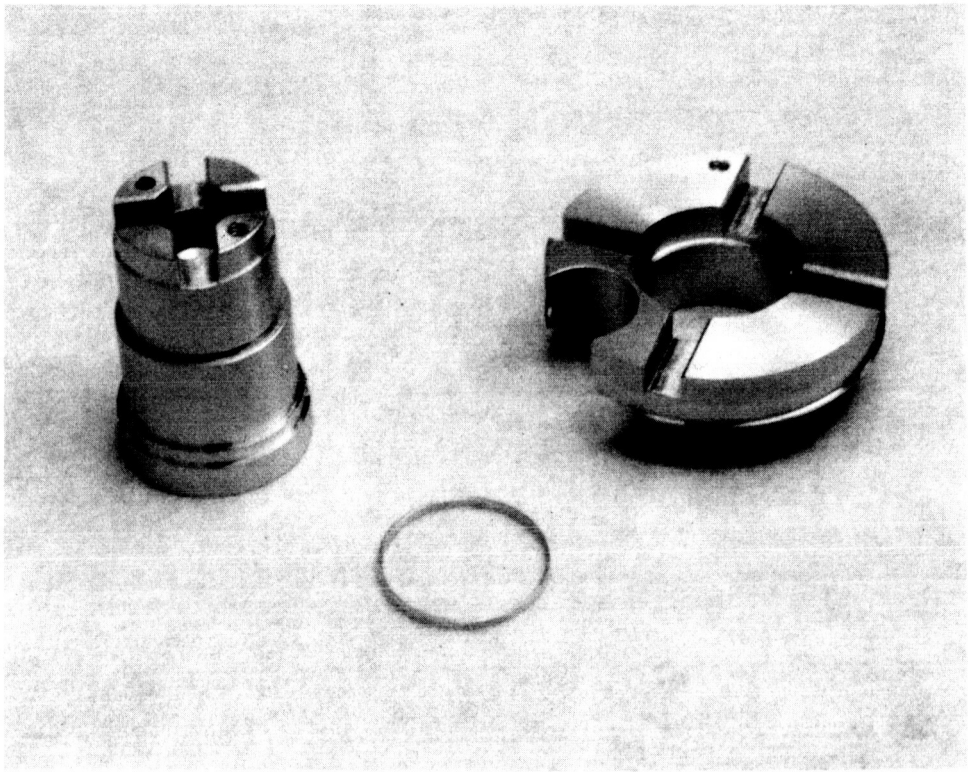

Figure 9. Parts for T-202 Collector Structure.

niobium palladium alloys showed that although palladium melts at 1552°C, a eutectic at atomic 50% palladium exists which has a melting point of 1560°C. It is therefore difficult to avoid producing this eutectic during brazing. To solve the problem, it was attempted to plate the palladium with enough copper to form a 10% by weight alloy of copper palladium. The melting point of this alloy would then have been 1454°C or practically 100°C lower than the melting point of palladium. When this was tried, it was found that the copper plating evaporated much too soon to provide any significant amount of copper at the presumed melting point of the copper palladium alloy. The collector of T-201 was finally brazed using pure palladium as a braze material but a tell-tale was used in order to provide a clear visual indication of the instant at which melting of the filler wire occurred. The procedure could not be repeated successfully for the assembly of converter T-202: small perforations through the niobium sleeve were present as a result of overalloying, and they were closed using copper as a braze filler. In the fabrication of converter T-203, it is intended to use simultaneously a 0.010" diameter wire of copper and a 0.010" diameter wire of palladium so as to form a copper-rich alloy of copper and palladium with a melting point sufficiently below that of palladium to avoid rapid alloying with the niobium. Later on, very thin shims of palladium will also be tried as a braze.

Figures 10 to 15 show the sequence of steps involved in the fabrication of the emitter structure, and no problems were encountered in the fabrication of this structure except in the case of converter T-201 where, because of a tight fit in the jigs, the parts were forced into position to such an extent that a mechanical misalignment resulted. It was found in inspection that the surface of the emitter was out of square with the axis of the support sleeve by a maximum of 4.4 mils. A similar check was made on the collector sleeve structure and it was found that the collector face was out of square by a maximum of 1.5 mils, thus leading to a maximum possible error of 5.9 mils prior to brazing of the seal in the

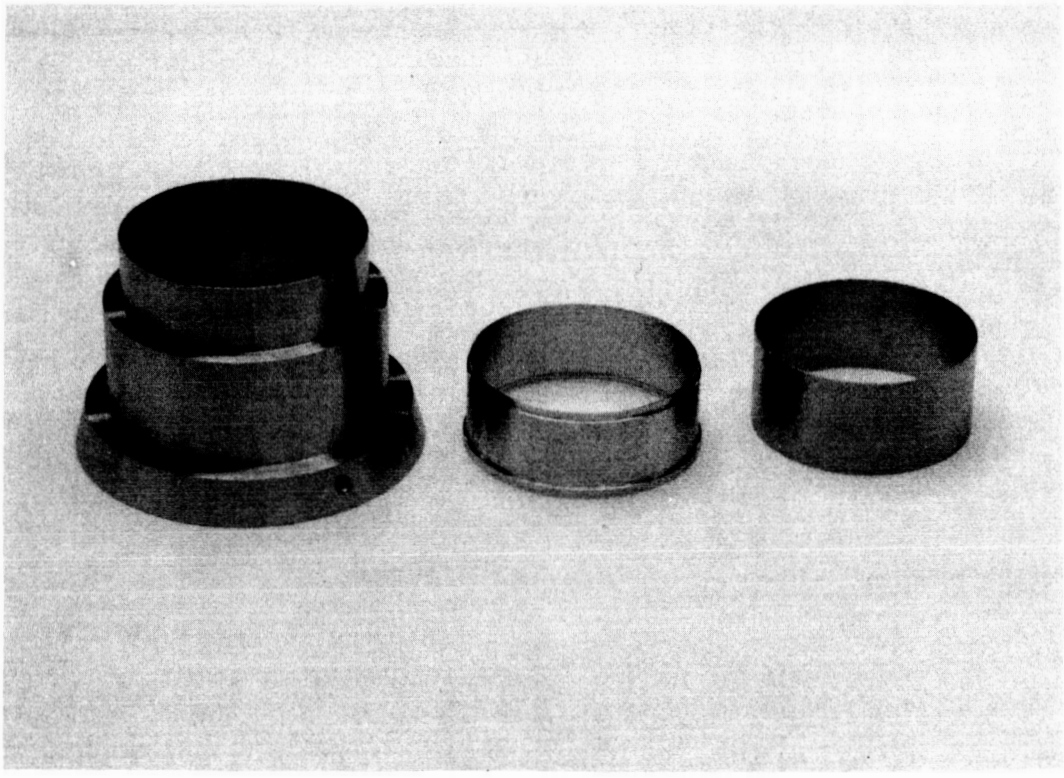

Figure 10. Parts for T-201 Emitter Support Structure.

Figure 11. First Weld of Emitter Support Structure.

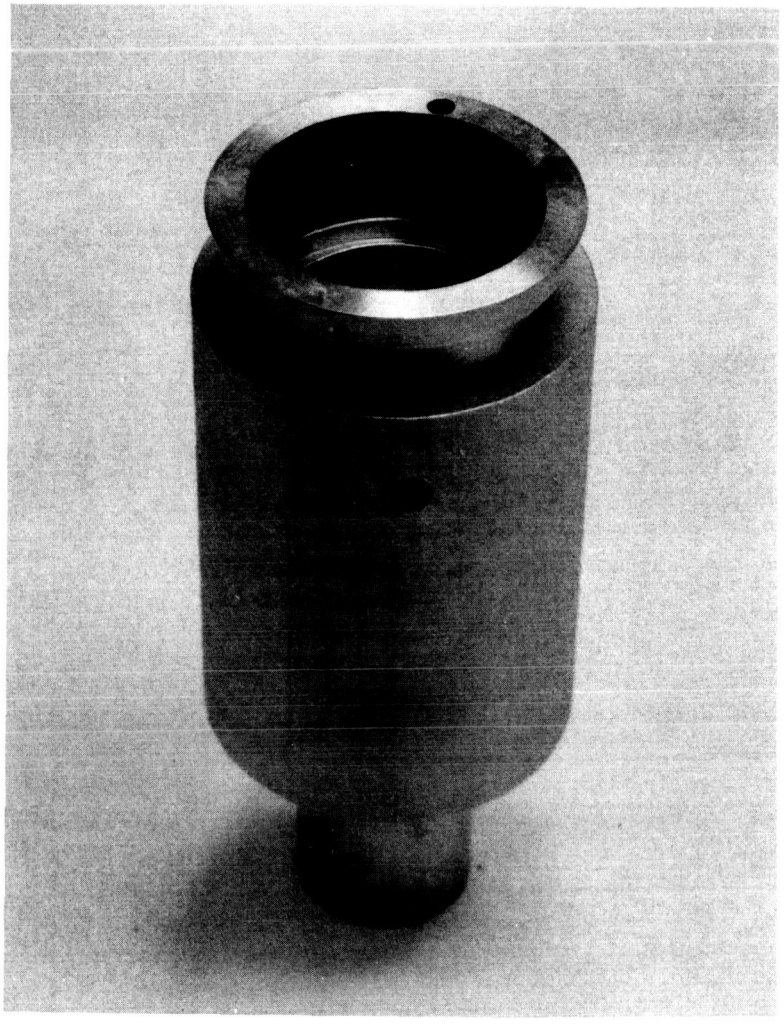

Figure 12. Second Weld of Emitter Support Structure.

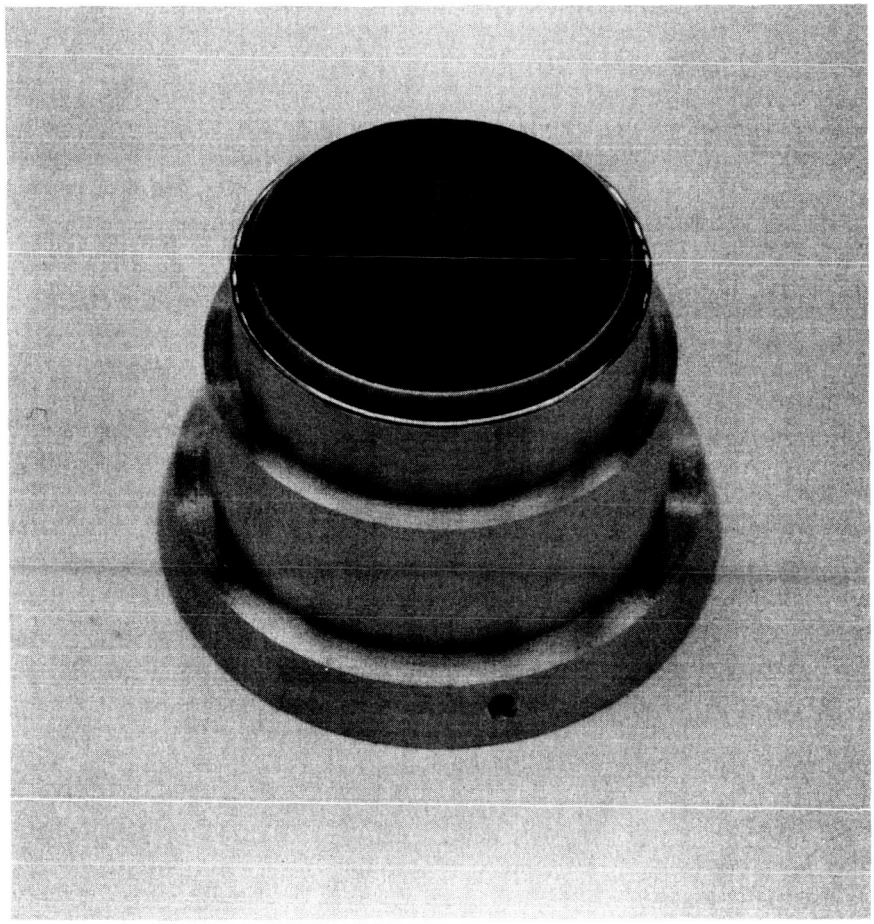

Figure 13. Finished Emitter Support Structure.

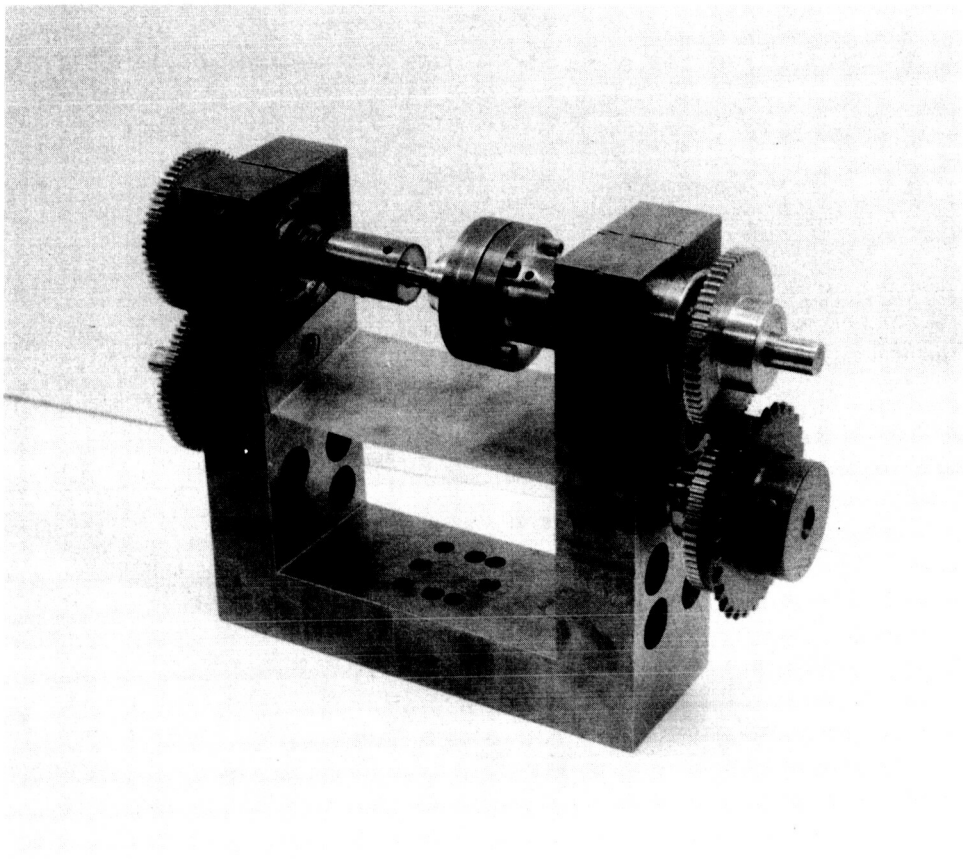

Figure 14. Emitter Assembly Ready for Electron Beam Weld.

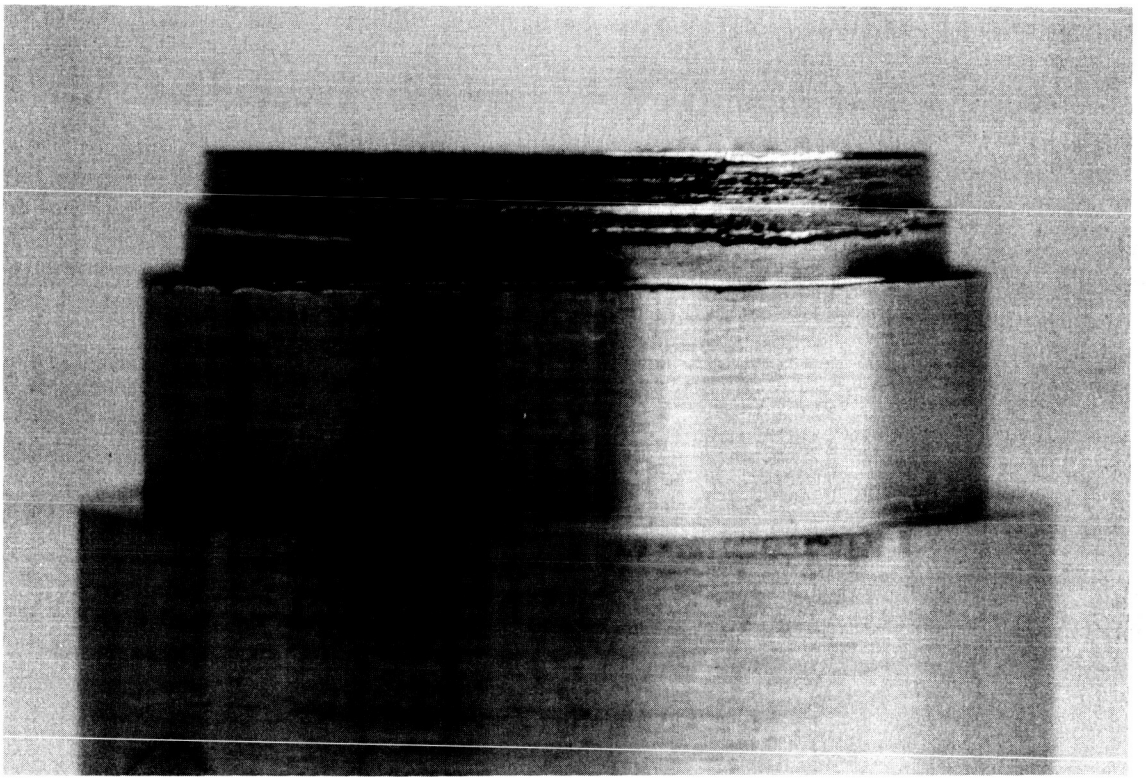

Figure 15. Weld Detail of Emitter Structure.

compression jig. Since the action of the compression jig represents a displacement which far exceeds the 5.9 mils, it was expected that the entire amount of the error should disappear during seal braze. Later cesium conduction tests on converter T-201 revealed that the design interelectrode spacing was not achieved, and it should therefore be considered that a misalignment condition such as that described above should result in rejection of the subassembly.

Figure 16 shows the parts for the seal braze assembled in the compression jig prior to brazing. Figure 17 shows the completed T-201 converter during cesium distillation. Cesium charging is achieved with 250 mg glass capsules heated to approximately 270°C during converter outgassing, prior to breaking, and then heating the cesium from the broken capsule, by means of two automatically controlled heaters, to 200°C for 5 hours.

The emitters of converters T-201, 202, and 203 were electroetched using the fixture shown in Figure 18. The fixture is a plastic structure which completely encloses the emitter piece and its attached current lead, except for the emitter surface which is made co-planar with the streamlined front-surface of the fixture. Thus, the fixture can be agitated in the electroetching solution without inducing cavitation or large scale turbulence which would otherwise interfere with uniform etching action. The time for electropolishing and electroetching was varied slightly to determine the duration that would cause a satisfactory action on the surface yet avoid excessive material removal and consequent departures from flatness. These tests showed that a 10-second electropolish and a 45- to 60-second electroetching should not be exceeded. Three emitter structures were electrolytically treated and then thermally stabilized. The treatment temperature for the T-201 emitter was limited to 1800°C for 20 minutes. The T-202 emitter was treated for one hour at 2400°C. As this second piece was removed from the furnace, it was observed that on the tantalum side large grain growth, partial

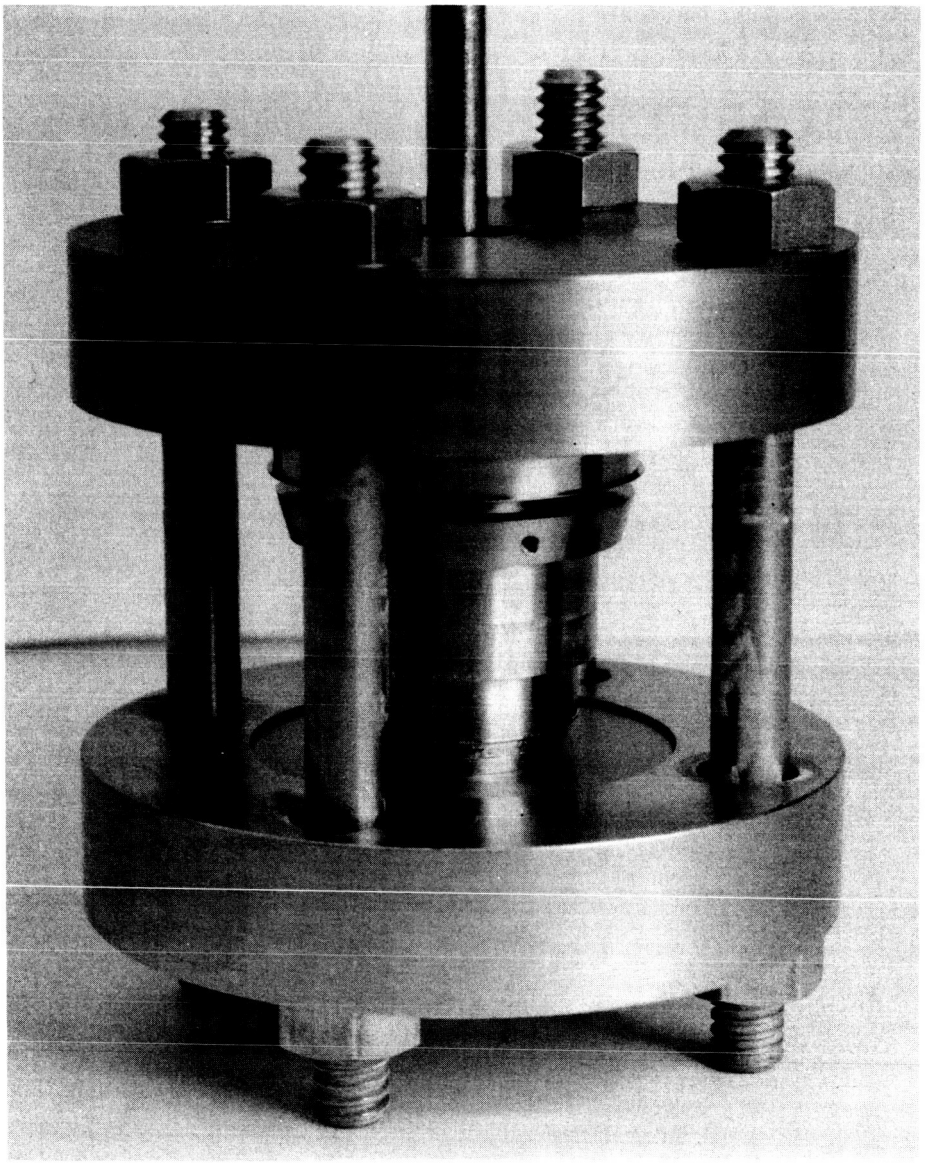

Figure 16. Parts for Seal Braze in Compression Jig.

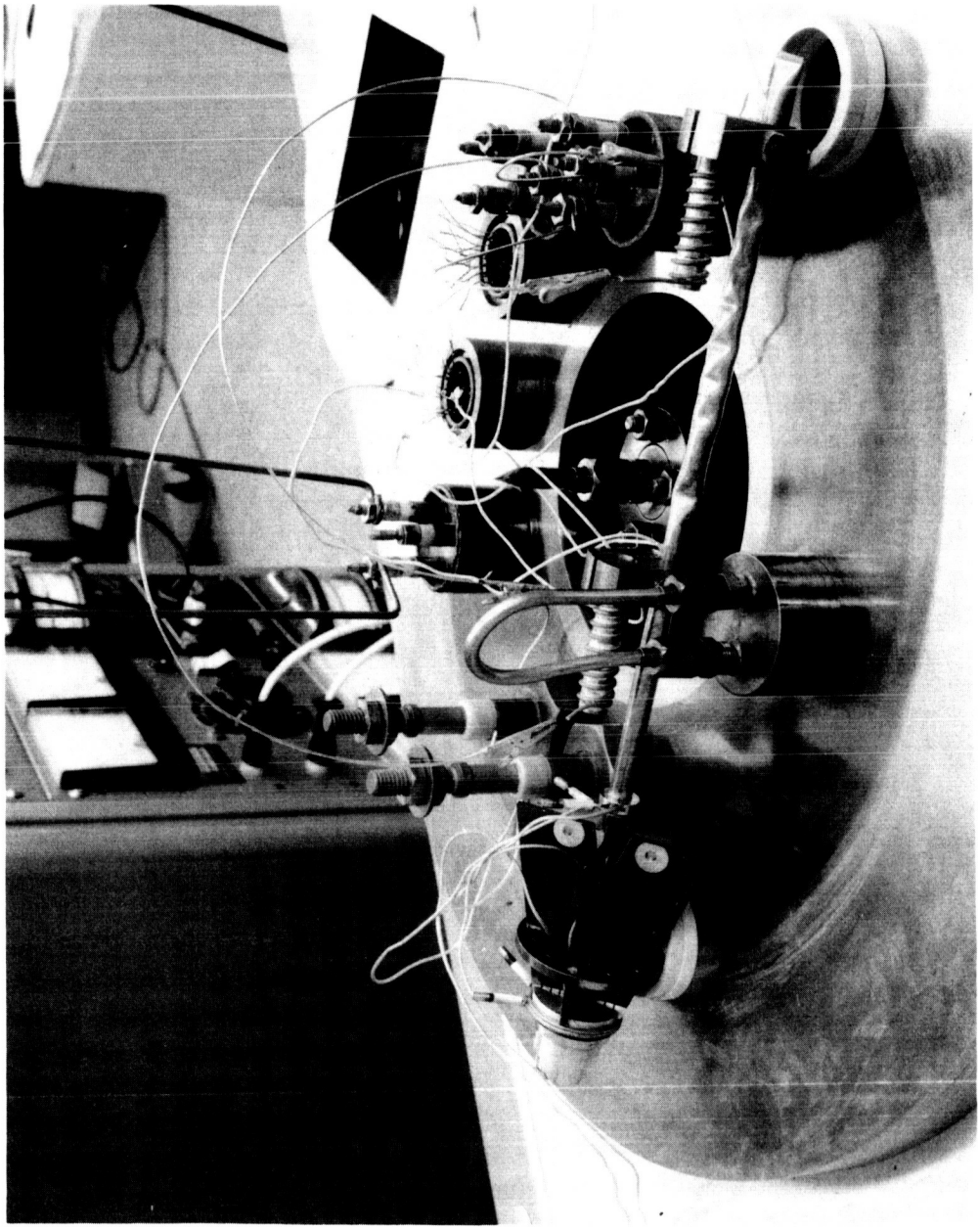

Figure 17. Cesium Distillation.

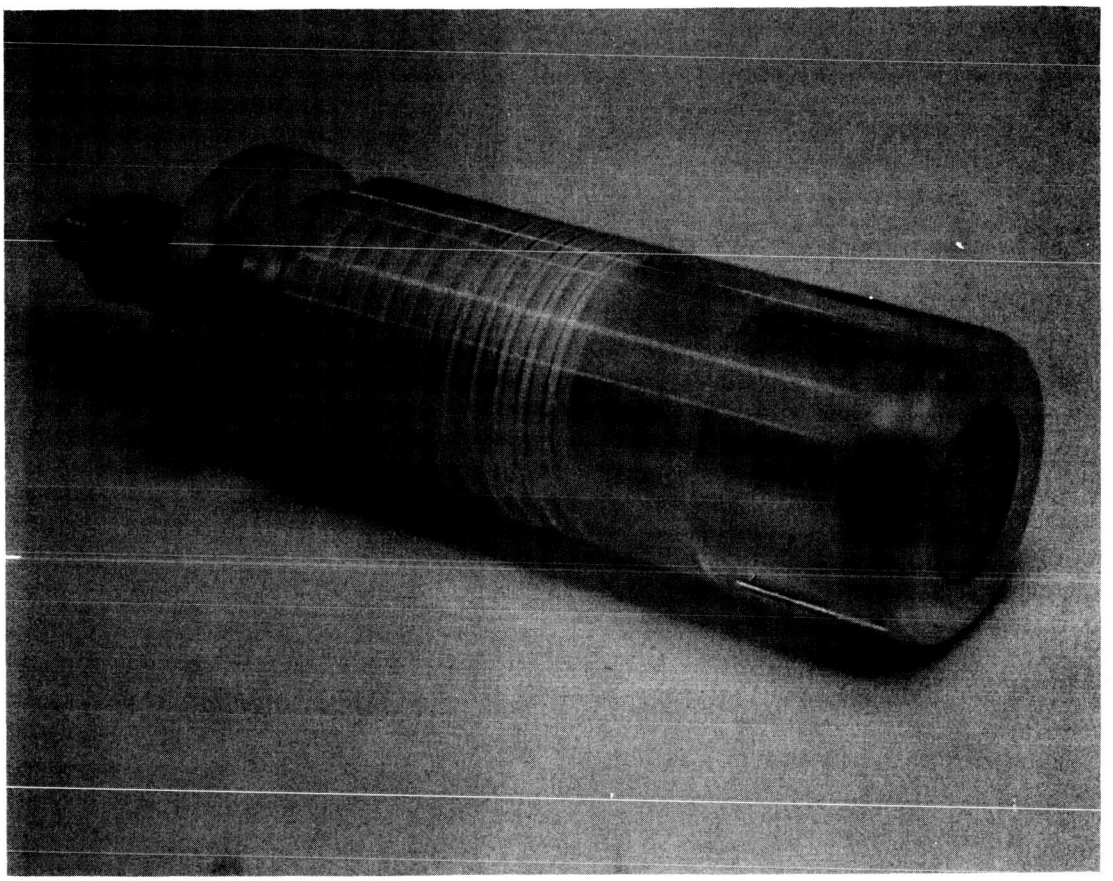

Figure 18. Emitter Electroetching Fixture.

melting and opening of the grain boundaries had resulted from the high temperature treatment. Consequently, the T-204 emitter was heat treated at 2100°C for one hour. Figure 19 shows the visual appearance of an electroetched emitter. Figures 20 and 21 show photomicrographs of the emitter surfaces of T-201 and T-202 after electroetching and heat treatment. Figure 22 is a view of the tantalum side of the T-202 emitter with the opening of grain boundaries and partial melting described above. Figure 23 is the photomicrograph of the T-203 surface.

The collector surface of T-201 was used with a ground finish. Converter T-202 used a surface chemically etched for 15 minutes. Figures 24 and 25 show the surface appearance after 5 and 15 minutes etching times. Because of some loss in flatness observed in the collector face of T-202 as a result of etching, it is intended to fabricate T-203 with a collector etched for only 5 minutes. Table 2 gives the observed tolerances in the emitter and collector structures of converters T-201 and T-202 and in the T-203 emitter structure.

1.4 Converter Testing

Converter T-201 has been fully tested and converter T-202 is presently in test. The test apparatus is essentially the same as that used in the performance of work under Contract 950671. To broaden the range of temperature control of the cesium reservoir, a water cooled copper strap is clamped to it. The test procedure is that outlined in JPL Engineering Note ADEN 342-005, and it consists of first making a relative collector work function measurement and sampling two I-V traces, then running under steady-state at a substantial output current for approximately 150 hours, making a new collector work function measurement, then proceed to evaluate the other converter characteristics by I-V curve and cesium conduction measurements, and finally testing the converter under state state conditions.

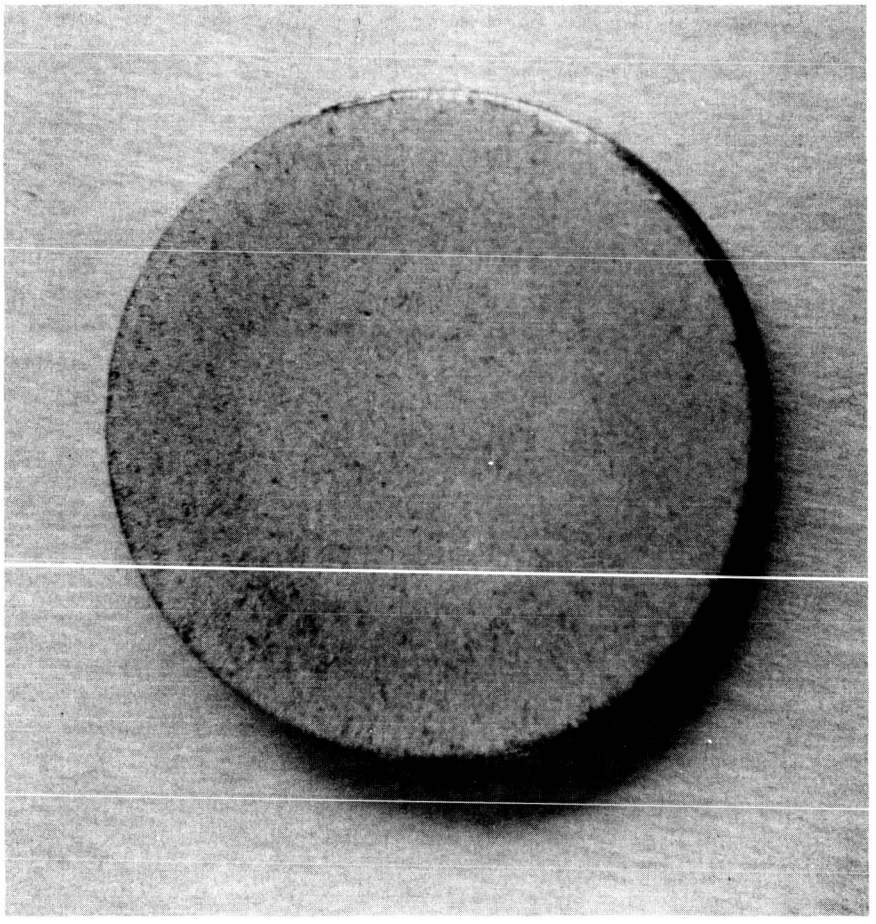

Figure 19. Visual Appearance of Electroetched Emitter.

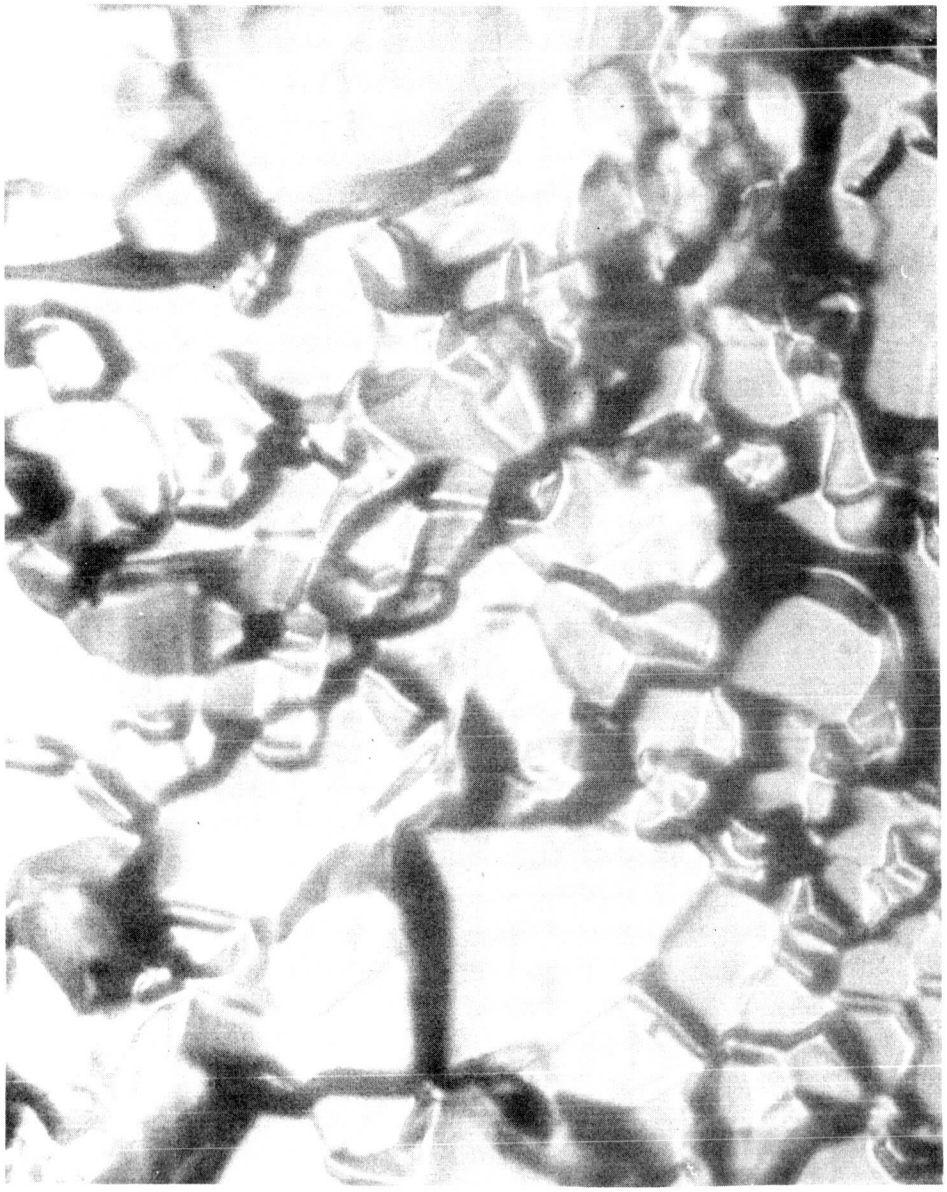

Figure 20. Photomicrograph of T-201 Emitter Surface (after 1800°C firing).

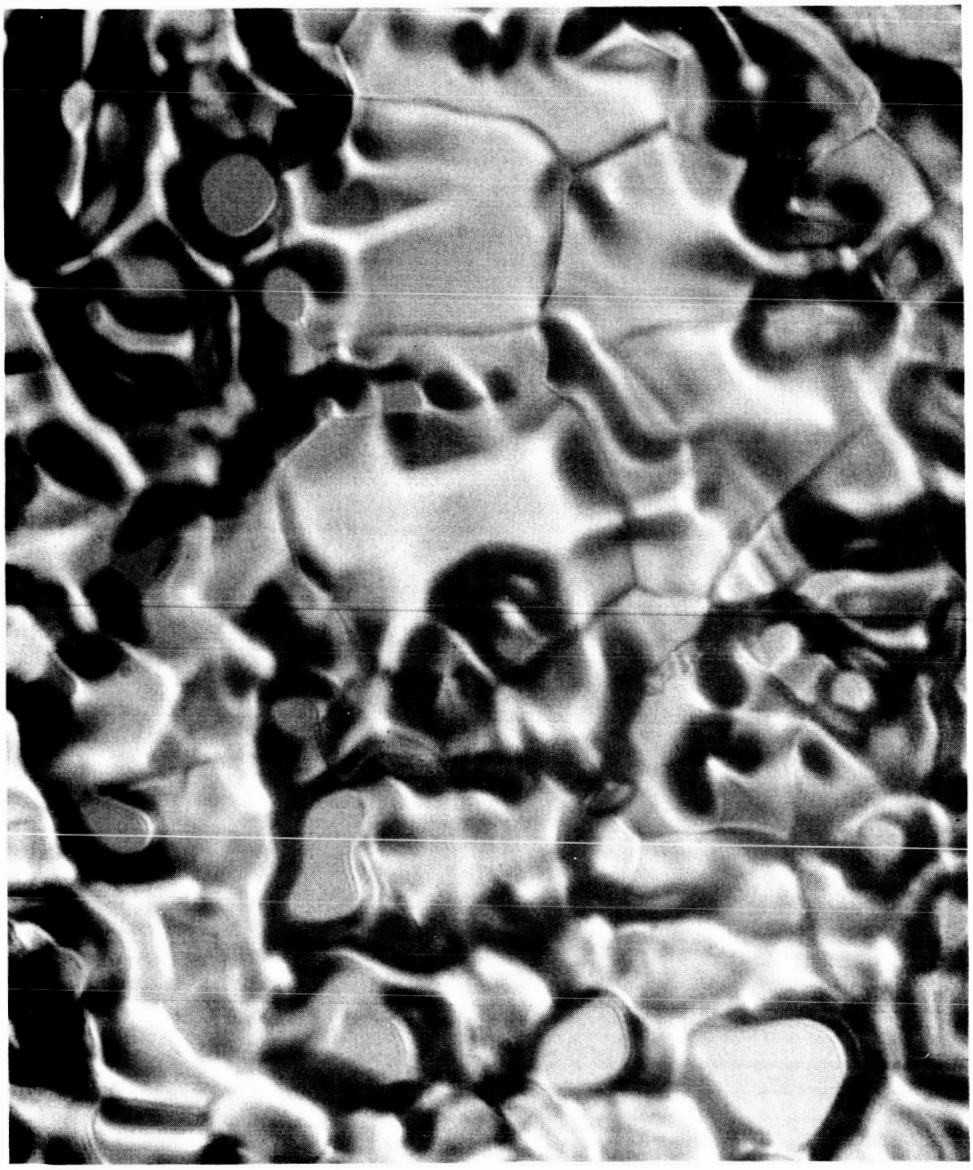

Figure 21. Photomicrograph of T-202 Emitter Surface (after 2400 °C firing).

Figure 22. Visual Appearance of T-202 Emitter Structure.

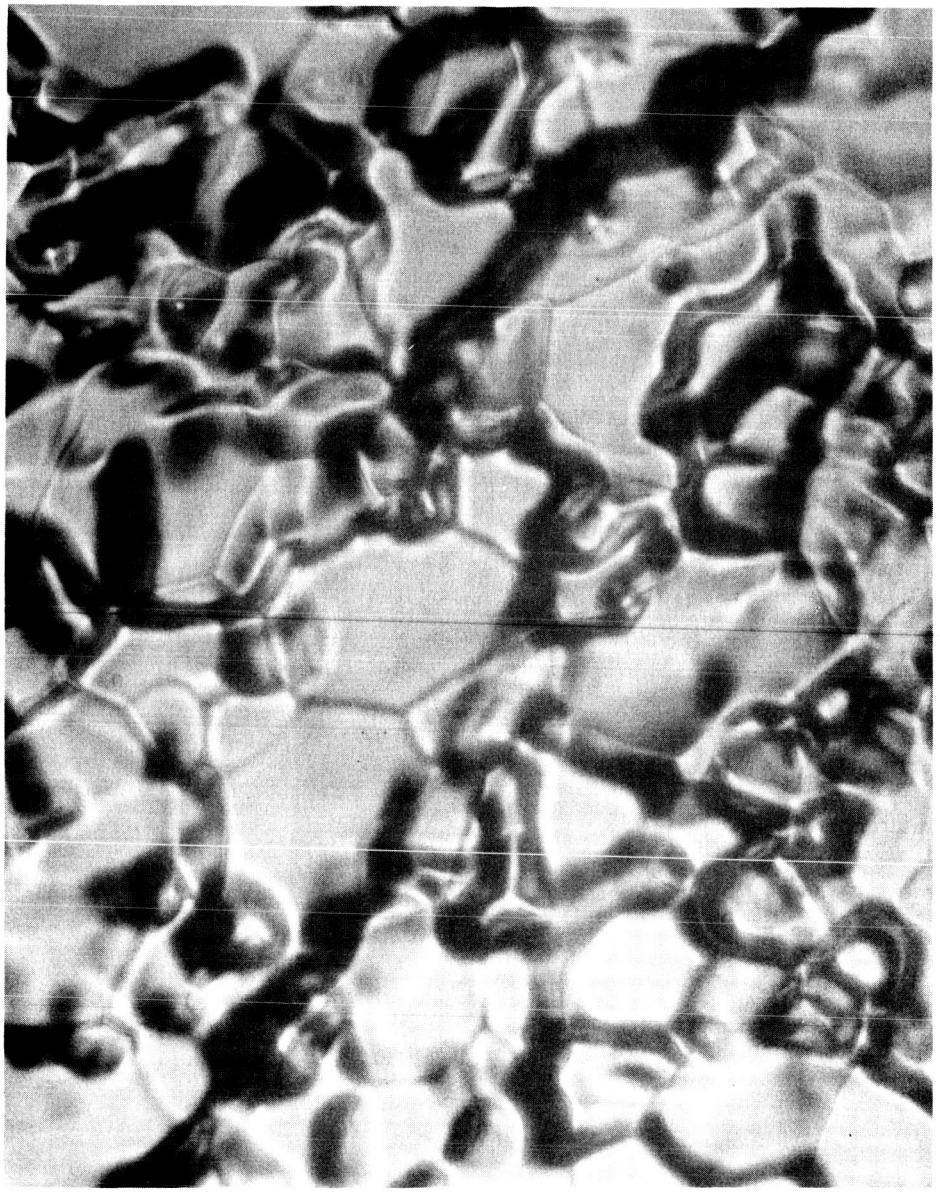

Figure 23. Photomicrograph of T-203 Emitter Surface (after 2100 °C firing).

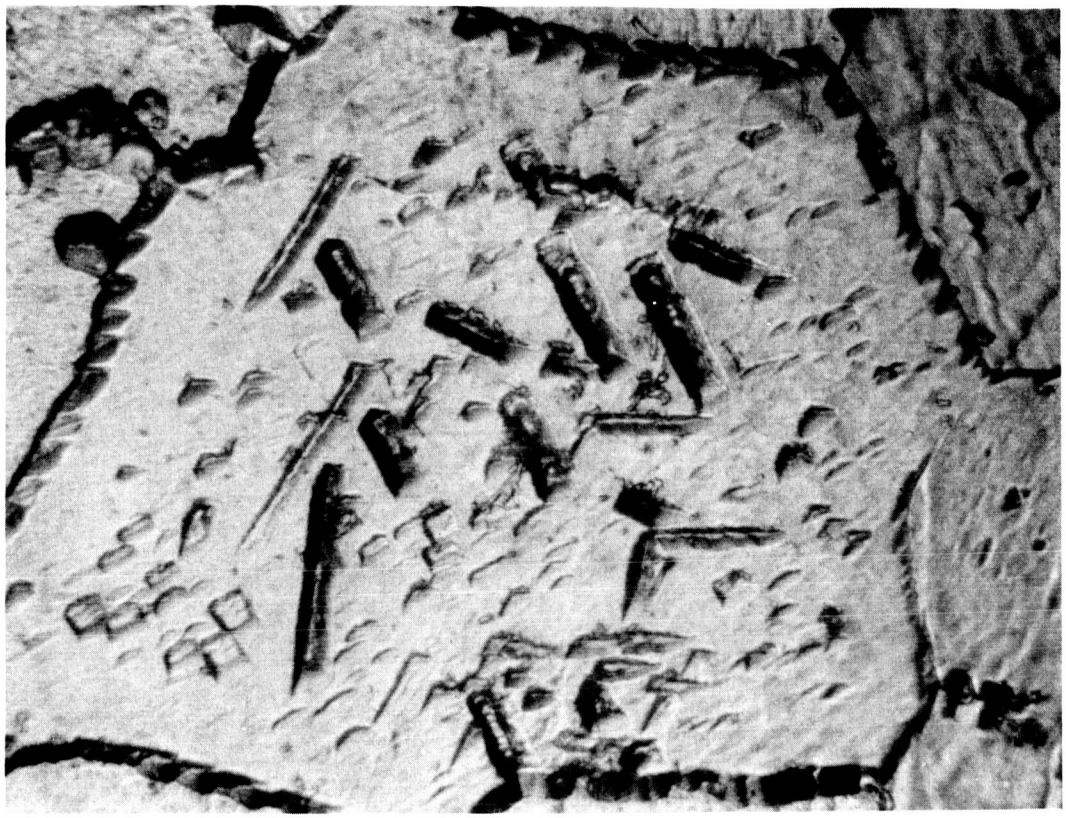

Figure 24. Photomicrograph of T-202 Collector Face (after 5 min. etch).

Figure 25. Photomicrograph of T-202 Collector Face (after 15 min. etch).

TABLE 2. SUMMARY OF OBSERVED ELECTRODE DIMENSIONAL TOLERANCES

Converter	Collector Structure		Emitter Structure	
	Out of Square	Out of Flat	Out of Square	Out of Flat
T-201	.0015	.0000	.0044	+.0003
T-202	.0013	+.0004	.0015	+.0004
T-203	—	—	.0003	+.0004

In the first four-hour operating period, it was not possible to obtain any output from T-201. The fact that the converter was able to deliver an open circuit voltage and not respond in any appreciable way to changes in reservoir temperature, indicated that the converter had no cesium in it. This was a surprising fact because the portion of the exhaust tubulation that had contained the fragments of the cesium capsule during distillation showed no cesium residues after distillation. The only way in which it appeared possible for the cesium to have escaped was to have dropped from the capsule into the converter exhaust pump right after cracking the capsule at the end of outgassing. This explanation was confirmed when the connections of the exhaust pump were disassembled and cesium residues were found in the pump manifold. Consequently, converter T-201 was opened, and it was further verified that the reservoir did not contain any cesium. The opening of the converter was effected at the pinch-off. The portion of the copper tube that corresponds to this pinch-off was removed to make room for connection of a new copper exhaust tube, and after replacement of the exhaust tube, the converter was outgassed and charged with cesium for a second time. During assembly of the new exhaust tube, the cesium heater was damaged at one of the terminals. It was decided to short this terminal to the cesium reservoir body, and use one of the radiator fins as a substitute electrical terminal.

Figure 26 gives the I-V characteristics obtained from converter T-201. The dashed lines represent the envelopes of dynamic measurements made at true emitter temperatures as indicated with optimized collector temperatures, and the solid lines give the steady-state outputs obtained at the true hohlraum temperatures indicated, with the collector allowed to reach its own equilibrium temperature, unaided by the electrical heater provided for collector temperature optimization. A comparison of these characteristics with those obtained from converter T-103 of the previous program shows that the current at large output

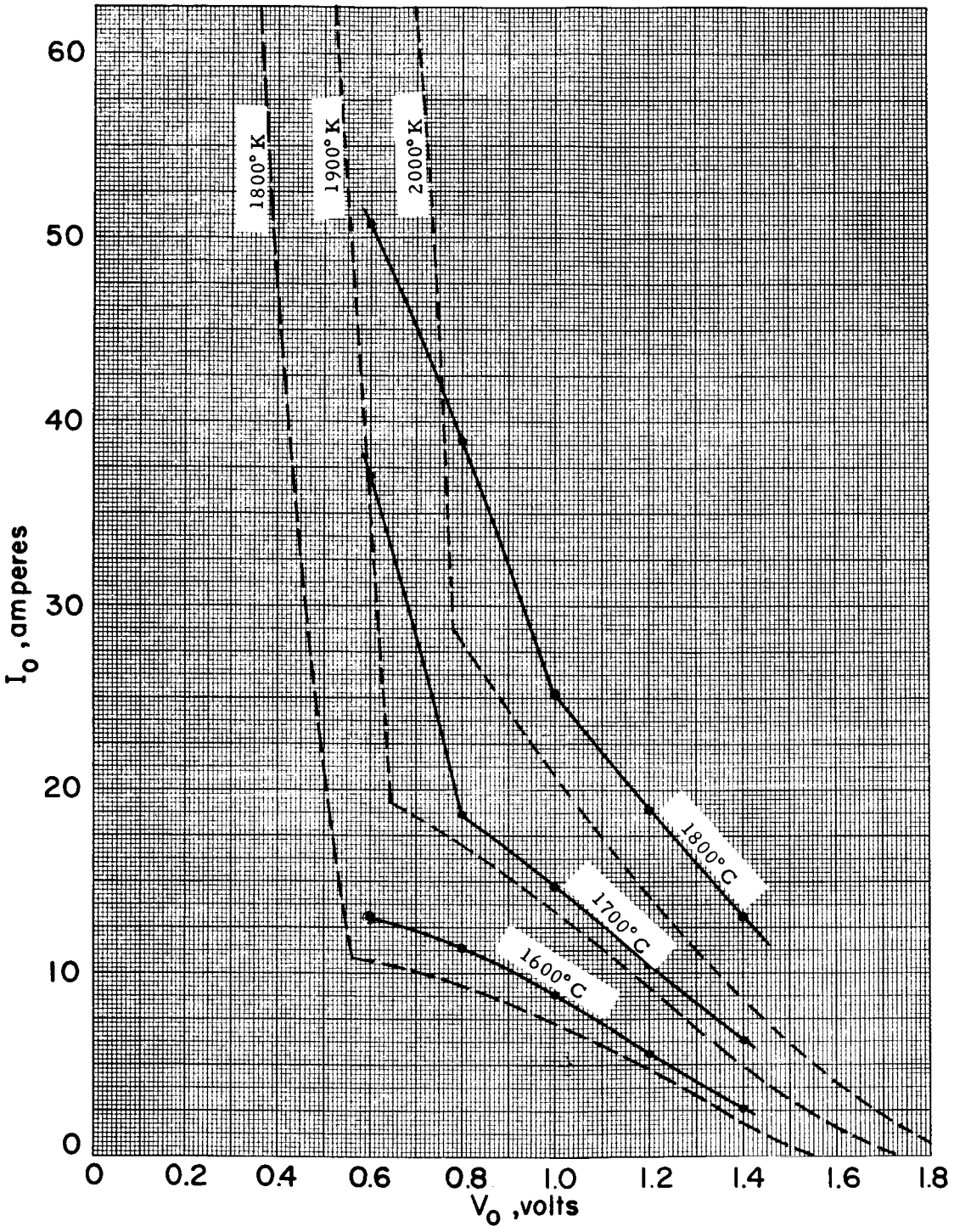

Figure 26. T-201 I-V Characteristics.

voltage (above 0.8 volts) has not been reproduced, and is smaller by approximately 30%. In fact, the converter T-201 performance resembles closely that of converter TE-104.

Cesium conduction experiments on converter T-201 later revealed that the interelectrode spacing was of the order of 1.4 mils as opposed to the 1.05 mils usually correlated by cesium conduction heat transfer measurements. As mentioned in Section 1.3, it is likely that this deviation is mostly due to the mechanical misalignment which was observed after using tight-fitting jigs. Poor performance of converter T-201 may also be related to the fact that, due to exceptional circumstances, the converter had to be re-opened and recesiated.

Initial tests of converter T-202 have shown that its output is appreciably better than that of T-201. The output current obtained during the steady state run of T-201 at 0.6 volts was 38 amperes. That of T-202 at the higher output voltage of 0.8 volts exceeds 40 amperes. Further data will be presented in the next quarterly report.

2.0 DESIGN OF MULTICONVERTER GENERATOR

2.1 Thermal Analysis

2.1.1 Cavity Geometry

For the purpose of conducting a flux distribution analysis, the generator cavity geometry was simplified so that a moderate number of parameters could describe it. The simplified geometry is shown in Figure 27, and, as is immediately apparent, it approaches very closely the actual cavity configuration. The major differences are:

1. Cavity interstitial spaces are lumped with cavity areas and treated analytically as sharing common average absorptivity and emissivity properties. Thus, the values of emissivity and absorptivity which are specifically assumed for the various cavity surfaces must take into account the fact that they include the properties of these interstitial spaces.

2. The shoe pieces of the converters are assumed to form a conical surface.

3. The faces of the converters are assumed to be flat and circular, and the shoe pieces are assumed to occupy the remainder of the cavity lateral area.

Figure 27 also defines the cavity nomenclature used. In all of the calculations, it has been assumed that the cone piece angle Θ, is equal to the concentrator rim angle of 52.5°. Also, except for finish on the heated surfaces, all converters were assumed to be identical, and of the T-200 design. The two families of converters shown in Figure 27 were given a tilt with respect to each other in order

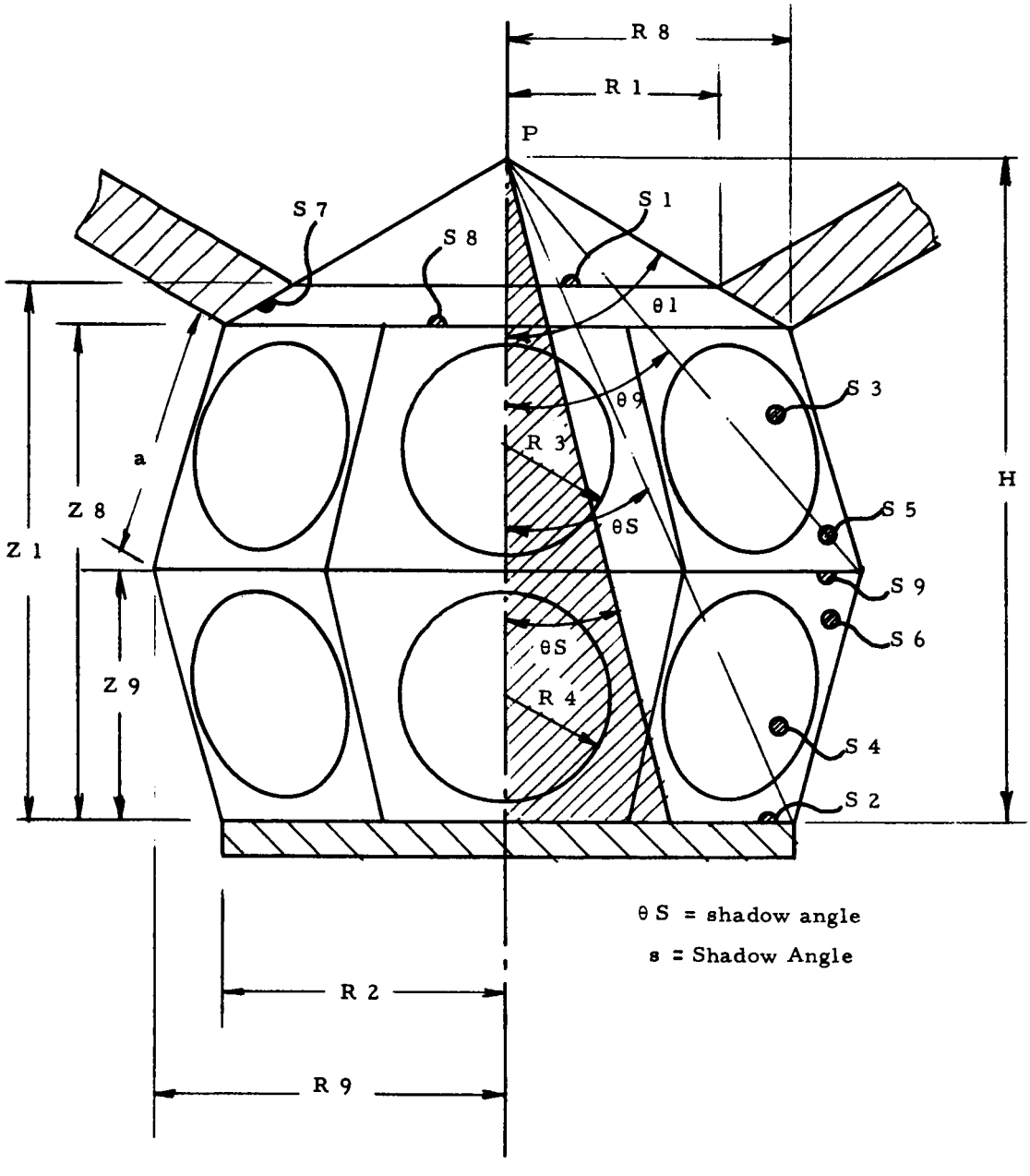

Figure 27. Cavity Nomenclature.

to accommodate the envelope of the converters, and the value of this tilt was equated to the minimum value allowed by the T-200 converter structure, namely 15°. The length to diameter ratio for the cavity corresponding to each selected number of converters was adjusted so that the size of the required converter shoe pieces was minimized.

2.1.2 Flux Distribution Analysis

One of the required data for the computation of the solar flux in the thermionic generator cavity is the actual amount of solar radiation that reaches the individual cavity elements considered in the analysis.

Since most cavity elements are reasonably removed from the focal plane, they will essentially " see" the arriving solar flux as though it had originated at a pseudo point source P on the optical axis, as shown in Figure 27, and with a specified polar distribution of intensity comprised between the rim angle Θ_1 of the concentrator and a shadow angle Θ_s produced by the generator and its test chamber on the solar concentrator.

Although the intensity produced by an ideal paraboloid increases slightly with Θ, the fact that profile errors also increase with Θ in actual concentrators has led to the assumption in this analysis that the solar flux is spread spherically with uniform intensity between the angles Θ_s and Θ_1. In all cases, Θ_s was assumed to equal 10°.

The reflection of both the solar flux and the cavity thermal radiation within the cavity was assumed to be diffuse. The view factors Fij between all seven areas Si of the cavity were calculated for each combination of number of converters and cavity aperture. Defining Ei and Ai as the thermal emissivity and solar

absorptivity of surface Si, each cavity surface i receives directly a solar input Wi, the fraction Fi of the total solar input W:

$$Wi = Fi * W$$

and it thermally radiates a flux per unit area:

$$Ei * Pi$$

where: $Pi = SIGMA * Ti ** 4$

and: SIGMA = 5.679 E - 12 (E = exponentiation)

If we denote by Vi and Hi the total thermal and solar fluxes arriving at each area i, the following matrix equations describe the cavity heat balance:

$$[Eij] * [Hi] = [Pii]$$

and $[Aij] * [Vi] = [Wi]$

where $[Pii] = [Fij] * [Ei * Pi * Si]$

$Eij = -Fij * (1. - Ei)$ for $i \neq j$

$Eij = 1 - (1. - Ei) * Fii$ for $i = j$

and Aij is obtained using the expressions for Eij and substituting Ai for Ei.

The net heat input at each surface is then:

$$Qi = Ei * (Hi - Si * Pi) + Ai * Vi$$

As it should be evident, the above calculations can be performed once the solar flux input is defined and the cavity temperatures are known. In all cases, the rear cavity surface temperature was assumed to equal the selected converter emitter temperature, and the cone piece temperature was arbitrarily assigned the value T7 = 1000°K. To describe the temperature distribution of the converter

shoe pieces these were assigned a single finite value of temperature which was found by computer iteration so that the temperature value would simultaneously satisfy the cavity flux distribution equations and the conduction heat transfer characteristics of the shoe piece.

2.1.3 Computer Program

Figure 28 shows the flow diagram of the computer program used to solve the flux distribution problem. The program was arranged so that the input data consists of the cavity aperture diameter, the solar flux input, the number of converters, the selected emitter temperature, and the emissivity and absorptivity of each surface element of the cavity. The computer then calculated the heat re-radiated by the cavity, the equivalent cavity emissivity, the heat absorbed by the rear cavity piece, the front cone piece and by each of the converters of each family, and the temperature reached by the shoe piece of each converter.

2.1.4 Concentrator Performance

As it is explained above, one of the required computer program inputs is the solar flux input corresponding to each value of cavity aperture. Two heat sources were considered: an 11.5 ft. dia. concentrator operated on Earth ground in conjunction with a protective pyrex window, and a 9.5 ft. dia. concentrator operated in cislunar space. In order to determine the net heat flux delivered to the cavity for these two cases, it was assumed that the relative flux intensity at the focal plane as a function of the ratio of position to theoretical solar image size would equal the values achieved in 5-foot concentrators. In addition, it was assumed that the concentrator reflectivity for the Earth case is 88%, and for the cislunar case, 89%; corresponding shadow losses assumed were 5% and 2%. A window loss of 11% was included in the Earth case. The resulting curves of cavity input flux vs. cavity aperture diameter are given in Figure 29.

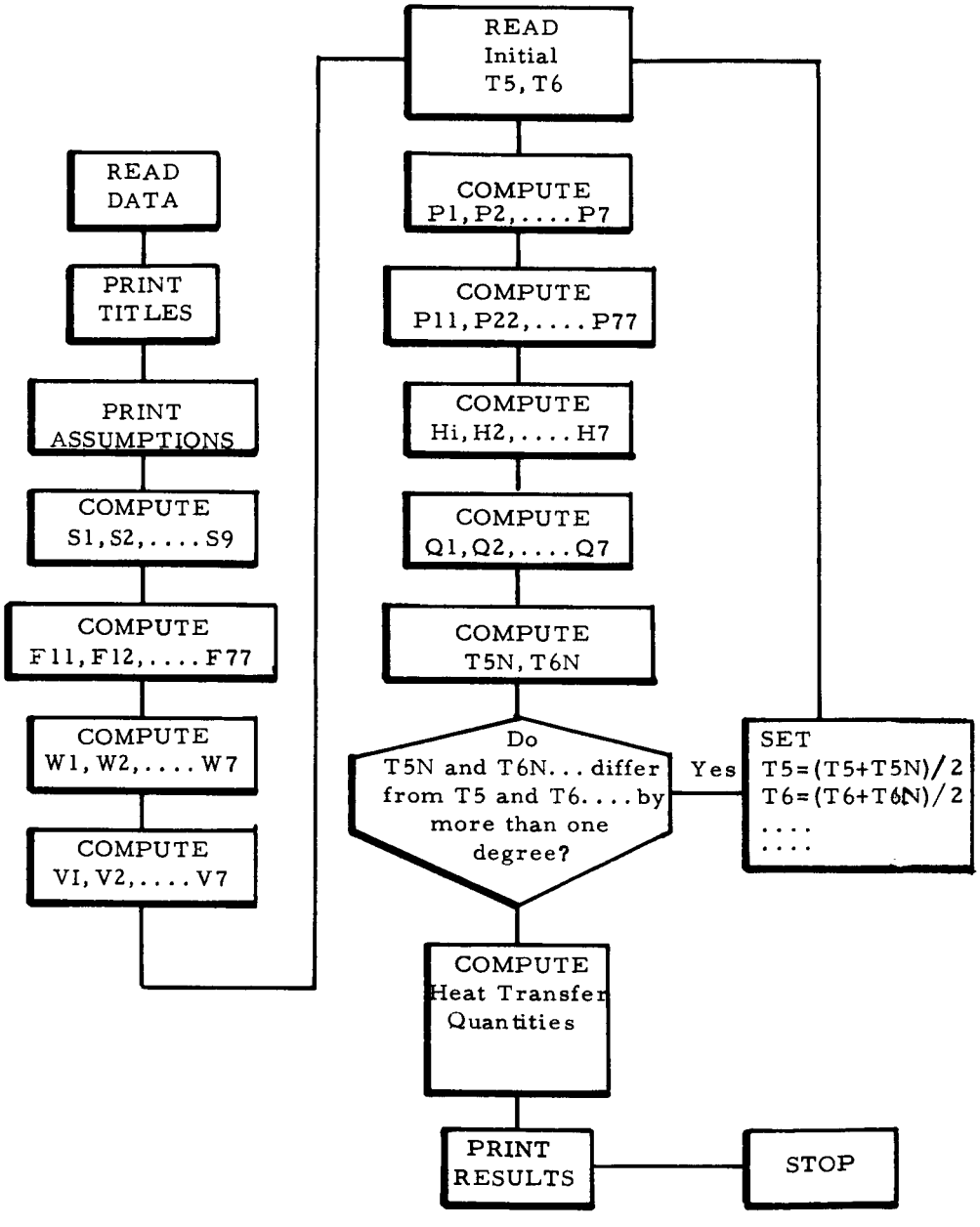

Figure 28. Computer Program Flow Chart.

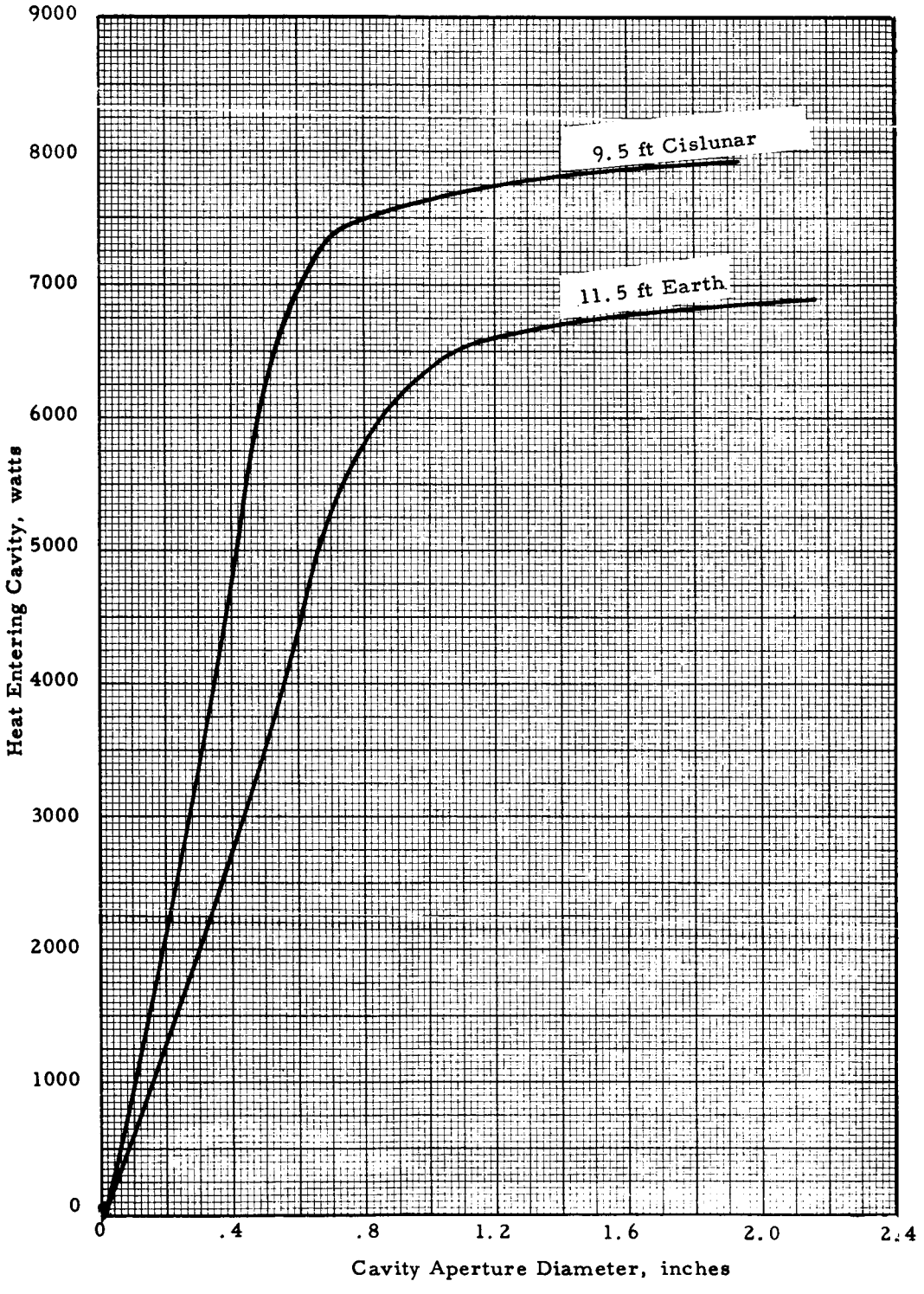

Figure 29. Assumed Concentrated Performance.

2.1.5 Predicted Thermal Performance of Generator Cavity

The flux distribution in the generator cavity was computed for 137 different conditions. In the first nine runs, the calculations performed aimed at evaluating the required emissivity on the heated faces of the converters to produce a balanced distribution of heat between the two families of converters. It was assumed that the emissivity of the heated face would be adjusted by grooving or etching the largest circle that can be inscribed on the heated face of each shoe piece, and that an increase in emissivity would be accompanied by a corresponding increase in solar absorptivity as predicted by the equations of radiation from v-grooves with diffuse surfaces. In the first nine runs, the chosen values of emissivity were 0.250, 0.400 and 0.563, and the corresponding values of solar absorptivity were 0.500, 0.750 and 0.875. All nine possible combinations of these three values were assigned to the two families of converters in a generator with 14 converters, a cavity aperture diameter of 1.400 inches, with the solar input corresponding to operation on Earth ground. The difference in the net heat transfer to the emitter structure of the converters of each family was then calculated, and it is plotted in Figure 30. The figure shows by extrapolation that, for the selected generator conditions, thermal balance is achieved for the values of E4 of 0.250, 0.400 and 0.563, provided the corresponding values of E3 are 0.145, 0.285 and 0.345 respectively. Since polished rhenium has an emissivity of approximately 0.250, the lowest possible value of E3 is 0.250, and Figure 30 shows by interpolation that the corresponding value of E4 for thermal balance is 0.365 to which corresponds a value of A4 of 0.700. Conversely, it was assumed that the highest value of A4 that can be achieved is 0.875 (corresponding to three reflections within the hit surface at a base absorptivity of 0.500) to which corresponds E4 = 0.563. The corresponding value of E3 at thermal balance predicted by Figure 30 is E3 = 0.310, and the corresponding absorptivity is A3 = 0.605.

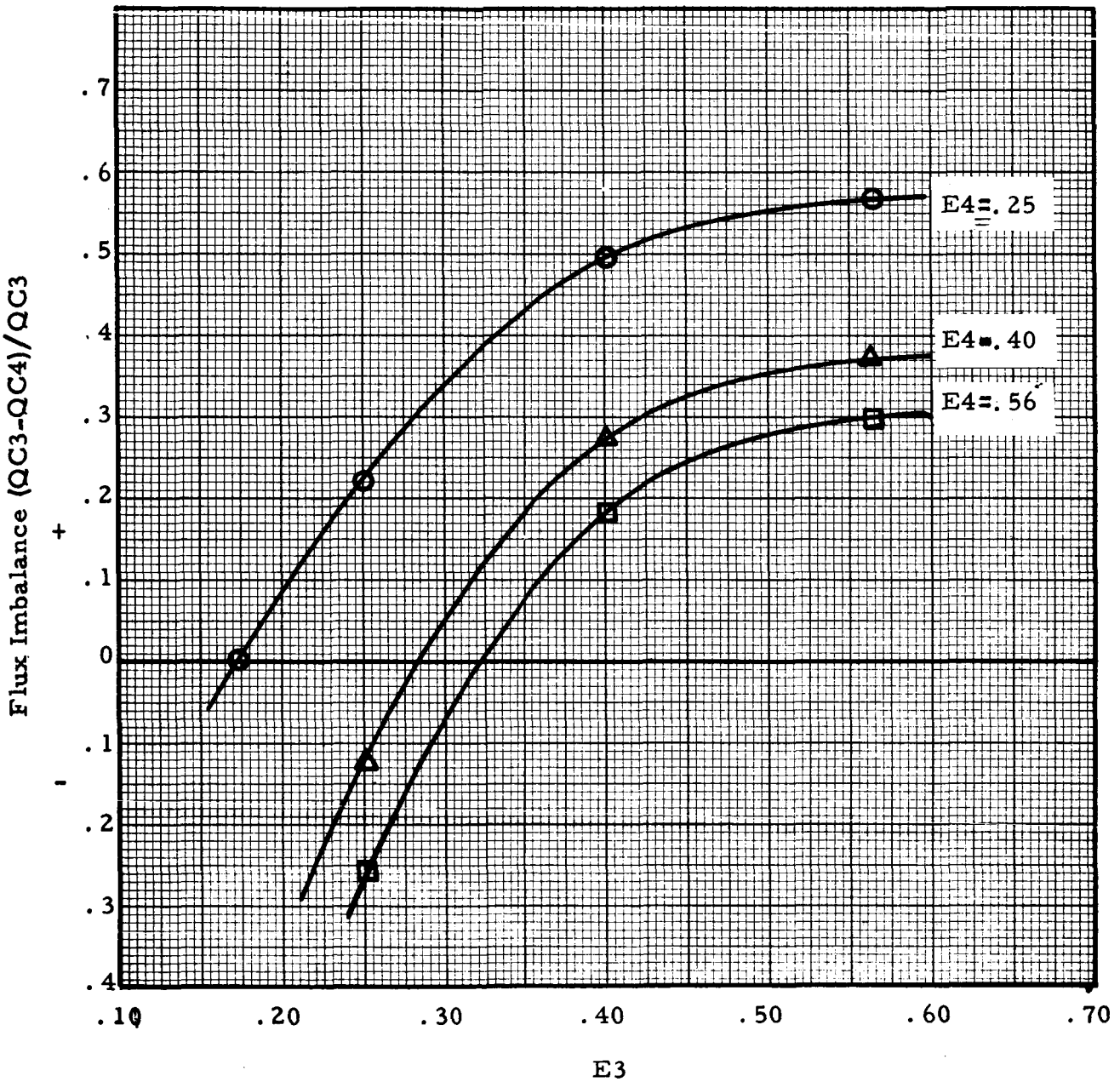

Figure 30. Effect of Surface Treatment on Flux Distribution.

In the next 64 runs, these two extremes of emissivity combinations were used to compute the thermal performance of generators with 10, 12, 14 and 16 converters, operated at 2000°K on Earth and in cislunar space, at four different values of cavity apertures. The results are plotted in Figures 31 to 34. It can be noticed in these figures that the large difference in emissivity conditions results in minor differences of thermal performance, and it is therefore possible to consider the use of the lower emissivity values which require the surface treatment of only one family of converters. Figures 31 to 34 are in ideal form for the later combination with the electrical performance curves of the converters in order to predict corresponding generator electrical outputs.

To determine the effect of changes in cavity temperature, 64 more runs were computed for 14 and 16 converter generators with the lower emissivity values (E3 = 0.250, E4 = 0.365, A3 = 0.500, A4 = 0.700), and operated both on Earth and in cislunar space with the converters at 1900, 2000, 2100 and 2200°K, at various cavity aperture diameters. The results of these runs are given in Figures 35 and 36. One of the most remarkable indications given by these two figures is that the 14-converter generator, which had been thermally balanced at Earth flux and for a cavity aperture of 1.4 inch, remains thermally balanced at the cislunar flux, at all emitter temperatures, and even over a wide range of aperture diameter variations. Although the 16-converter generator is not as closely balanced for the emissivity values selected, it should be noted that in the case of greatest imbalance, the heat QC3 received by the front converters exceeds that received by the rear converters by less than 10%.

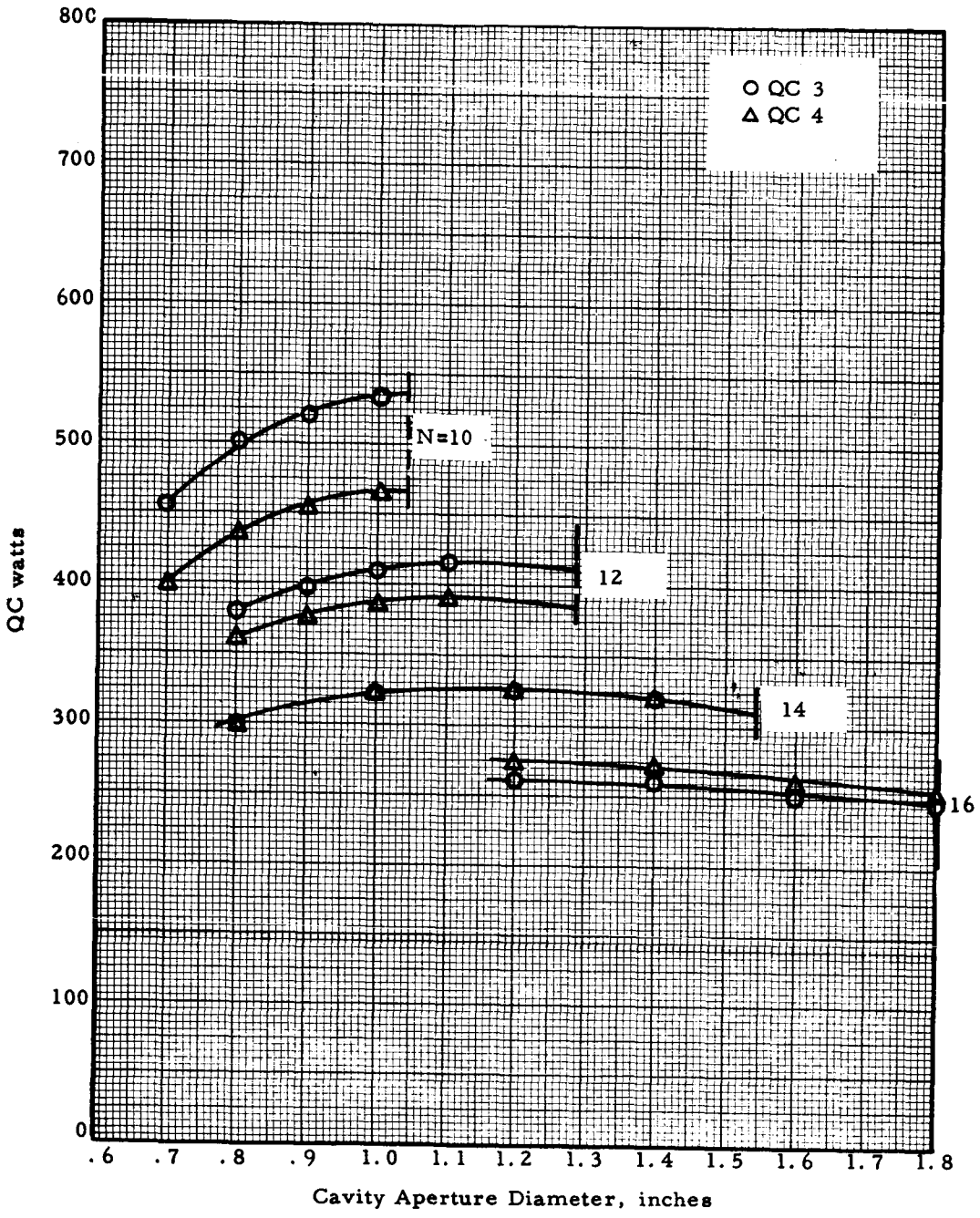

Figure 31. Predicted Cavity Performance at Low Emissivity - Earth Case.

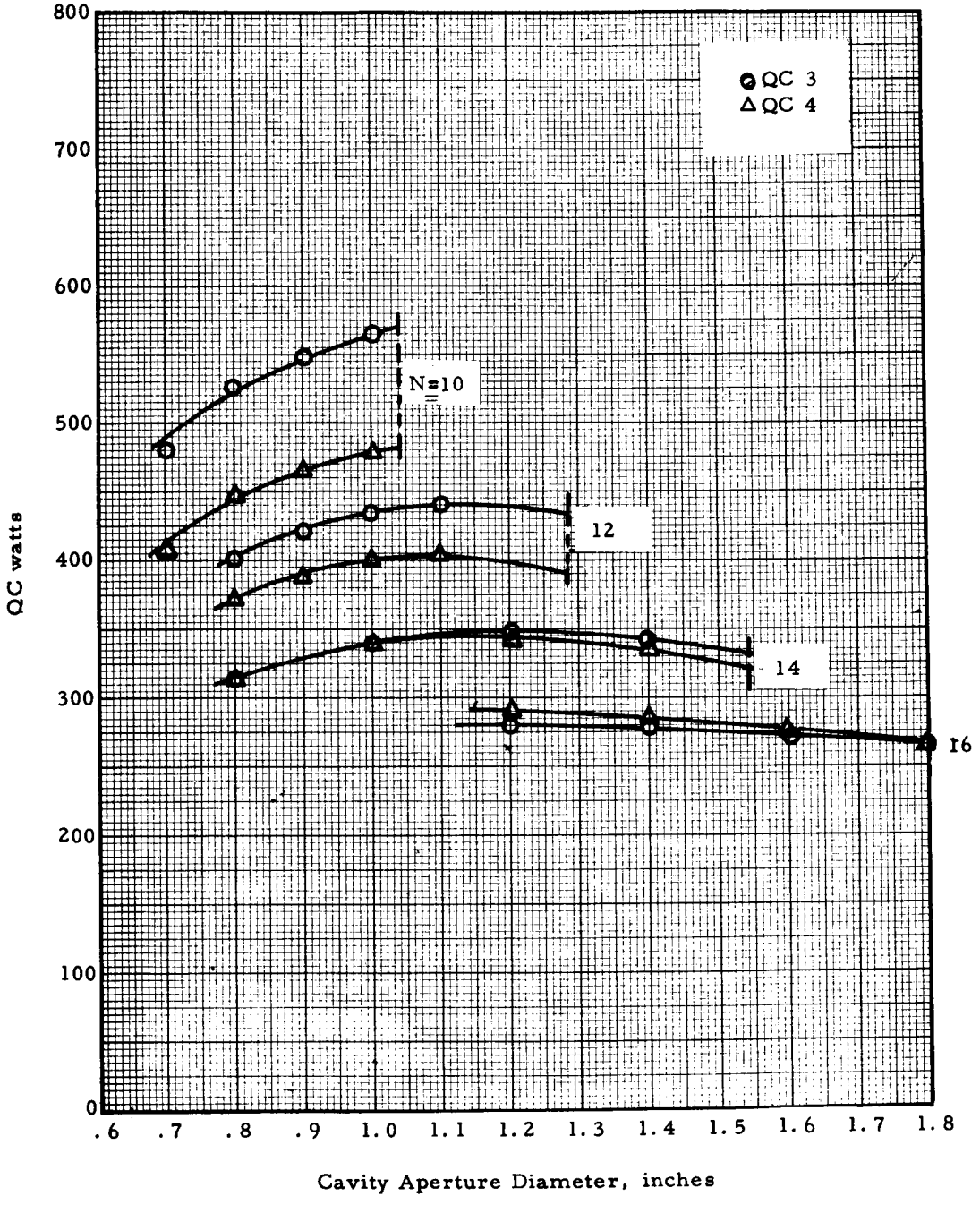

Figure 32. Predicted Cavity Performance at High Emissivity - Earth Case.

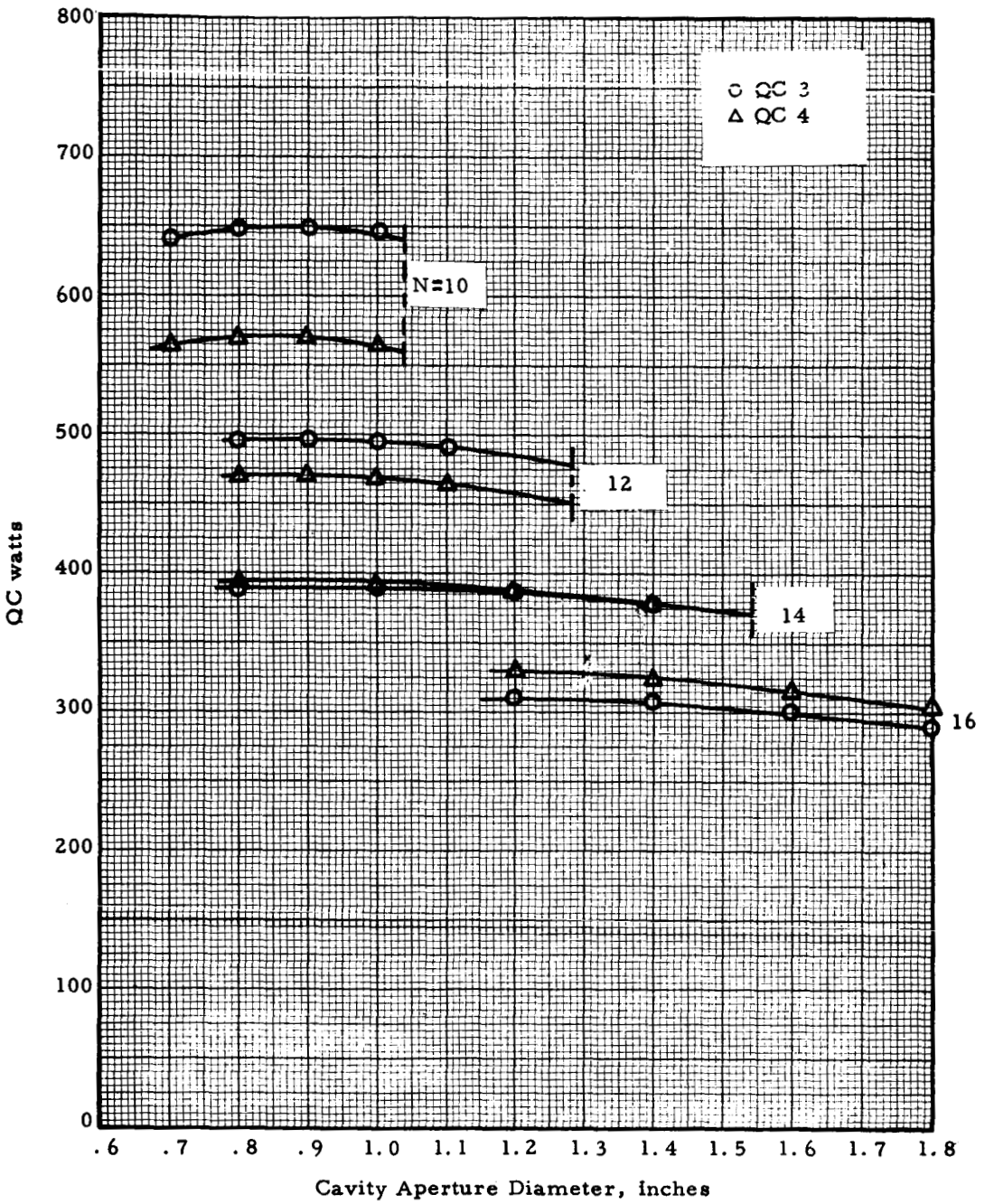

Figure 33. Predicted Cavity Performance at Low Emissivity - Cis lunar Case.

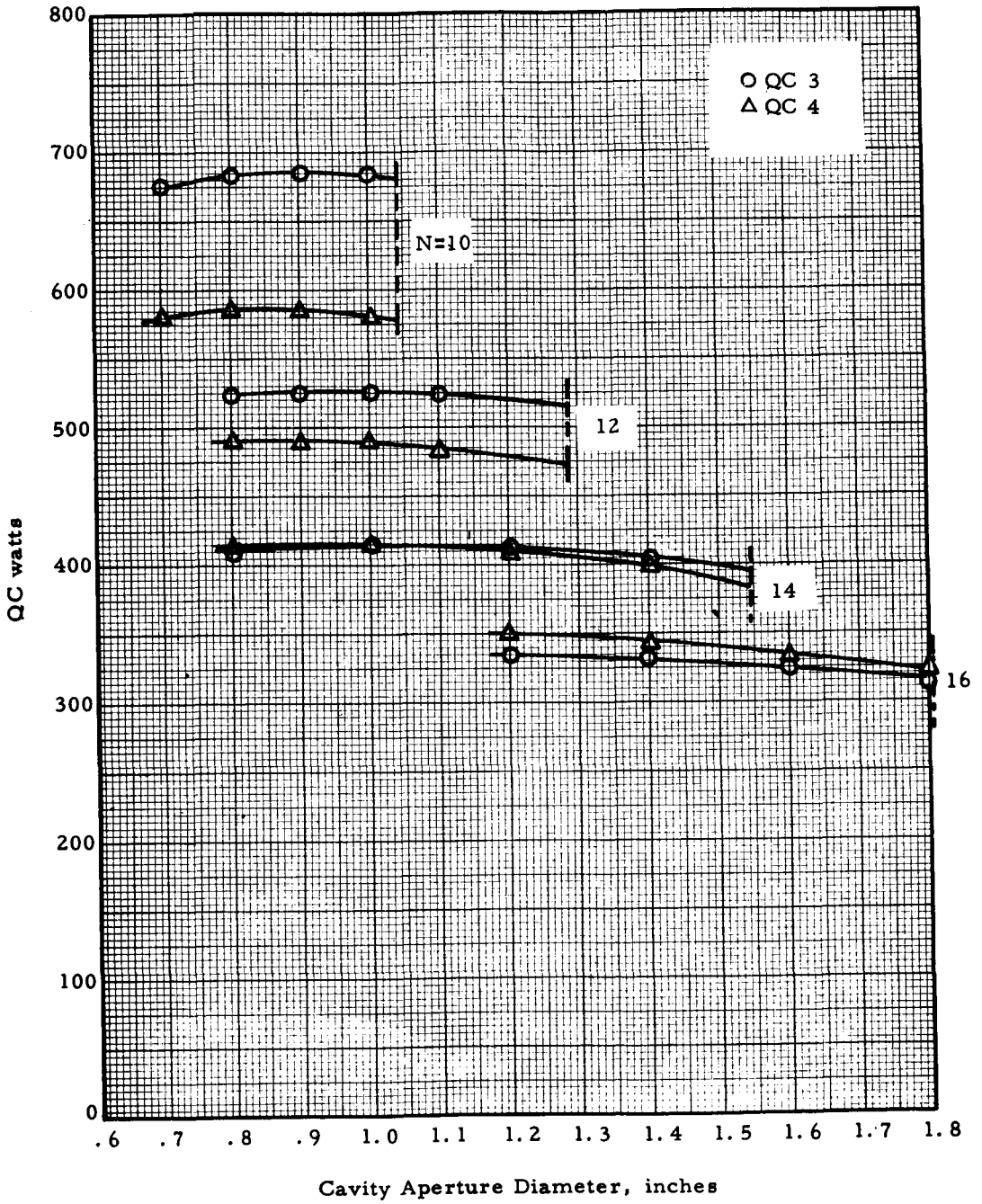

Figure 34. Predicted Cavity Performance at High Emissivity - Cis lunar Case.

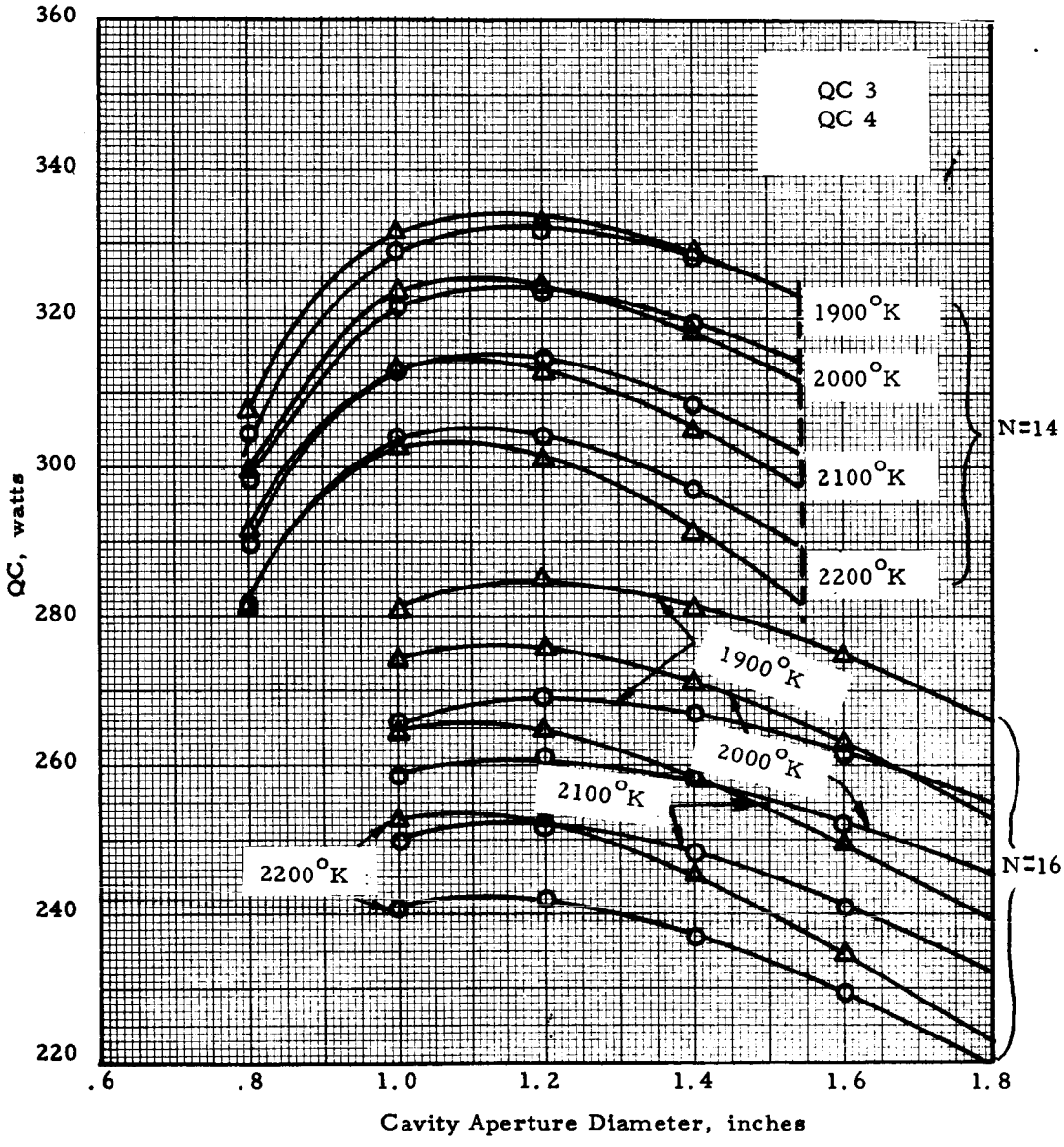

Figure 35. Effect of Cavity Temperature - Earth Case.

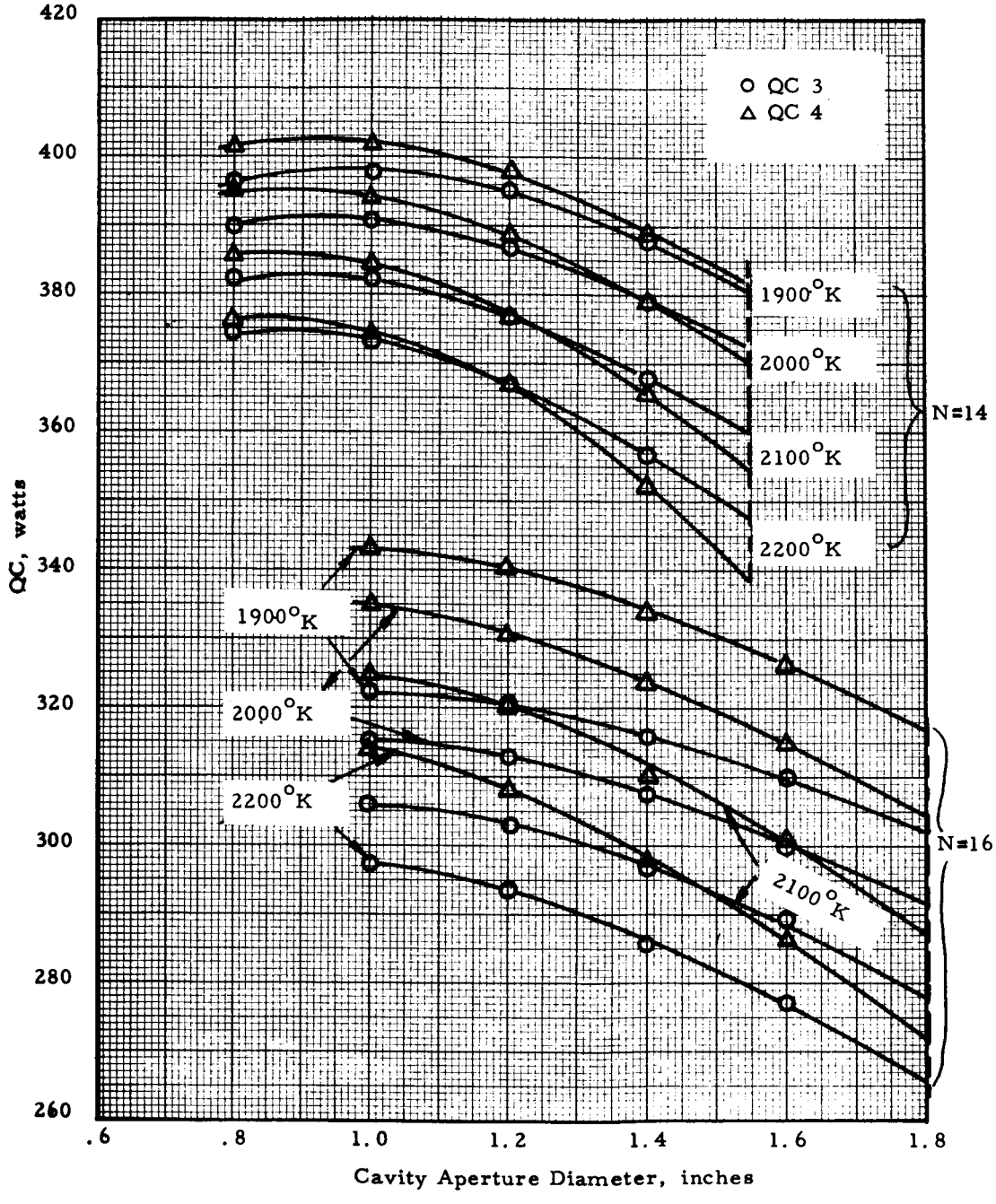

Figure 36. Effect of Cavity Temperature - Cislunar Case.